



Science case for 0.9-2.5 μ m infrared imaging with the VLT.
ESO /STC-323

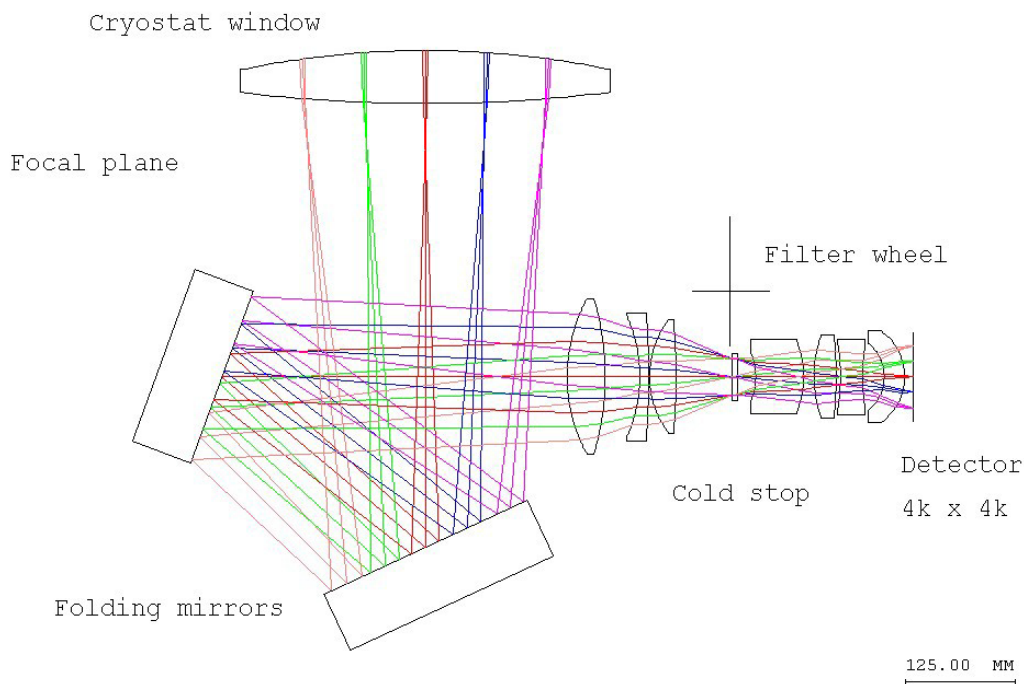


EUROPEAN SOUTHERN OBSERVATORY

VERY LARGE TELESCOPE

2nd Generation Instrumentation

Science case for 0.9-2.5 μ m infrared imaging with the VLT



March 18th 2003

**Prepared by A. Moorwood
with contributions from**

**W. Brandner, F. Comerón, E. Daddi, B. Fort, E. Giallongo, P. Grosbøl,
O. Hainaut, T. Henning, C. Lidman, M. McCaughrean, A. Renzini, G. Rudnick,
L. Wisotzki**



CONTENTS

1. SCOPE.....	2
2. INTRODUCTION AND BACKGROUND	2
3. THE BASIC CASE FOR 0.9-2.5μ IMAGING AT THE VLT.....	4
4. SELECTED SCIENCE CASES	5
4.1 Galaxy Evolution from Deep Multicolour Surveys	5
4.2 Multi-wavelength Observations of Normal and Active Galaxies.....	18
4.3 Structure and Evolution of Nearby Galaxies	19
4.4 Galactic Star and Planetary Formation.....	20
4.5 Outer Solar System Bodies	35
5. REFERENCES.....	37



1. Scope

This document presents a scientific case for retaining and expanding the capability for near infrared (0.9-2.5 μ m) direct imaging at the VLT by building a dedicated camera (HAWK-I) to replace ISAAC (and probably SOFI at the NTT) within the next few years.

2. Introduction and Background

Near infrared direct imaging is currently offered by SOFI at the NTT and ISAAC at the VLT. SOFI covers the wavelength range 1-2.5 μ m and offers fields of $\sim 5 \times 5'$ with 0.29" pixels or $\sim 2.5 \times 2.5'$ with 0.14" pixels. ISAAC covers the range 1-2.5 μ m over a field of $2.5 \times 2.5'$ with 0.147" pixels and the 2-5 μ m range over $70 \times 70''$ with 0.07" pixels.

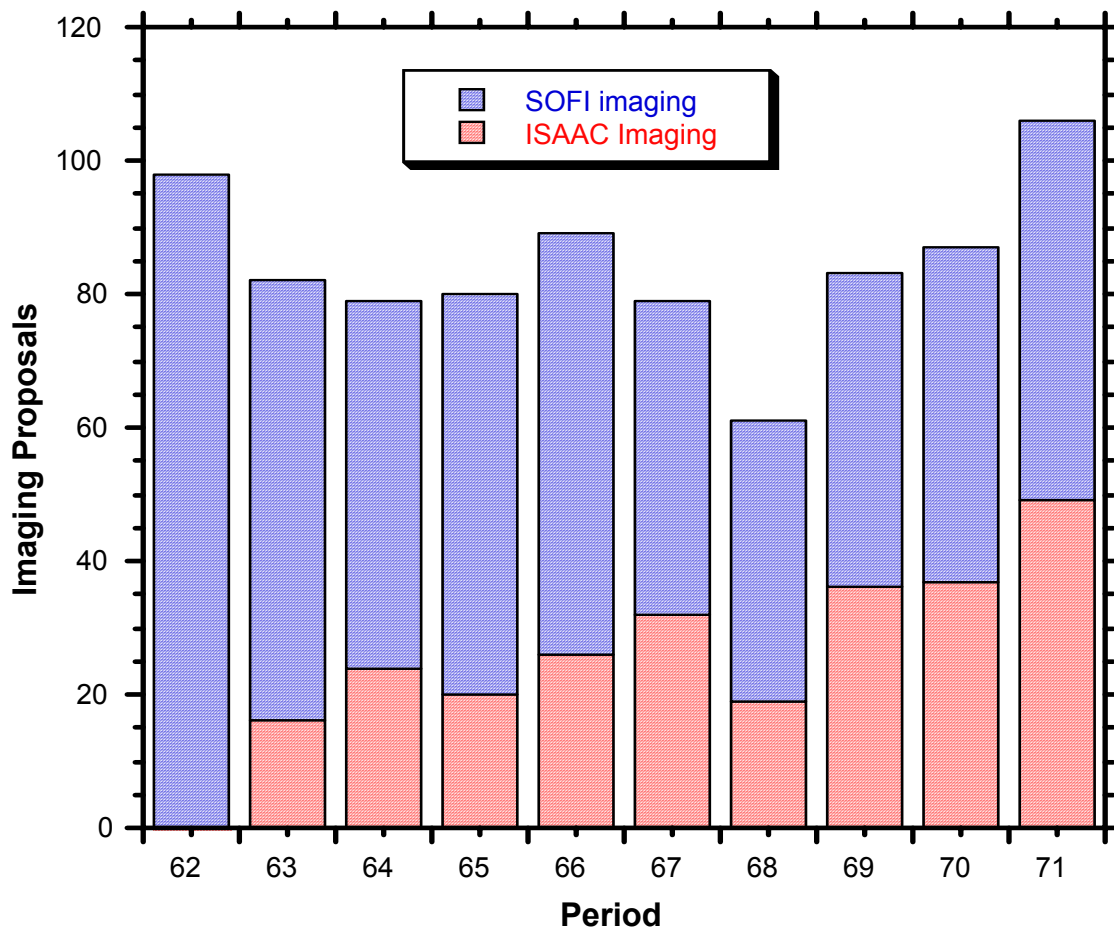
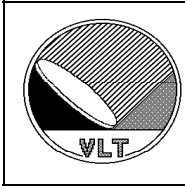


Fig. 2.1 Imaging proposals for SOFI and ISAAC from Oct 1998 to Oct 2002.

Over the last 5 years the combined demand for imaging with both instruments (both also offer spectroscopy which is not considered here) has remained high and roughly constant



but with a steady increase in the ISAAC share as shown in Fig. 2.1. Actually demand rose slightly in P71 despite the fact that NACO, which provides 1-5 μ m adaptive optics assisted imaging and spectroscopy, was offered for the first time and also attracted a large response.

Fig. 2.2. is a histogram of all the archived SOFI and ISAAC frames obtained in imaging programmes in both broad and narrow band filters up to Feb. 2003. Of interest is that the highest demand by far has been for the Ks filter and that use of the wide range of narrow band filters has been relatively modest compared with broadband J,H,K.

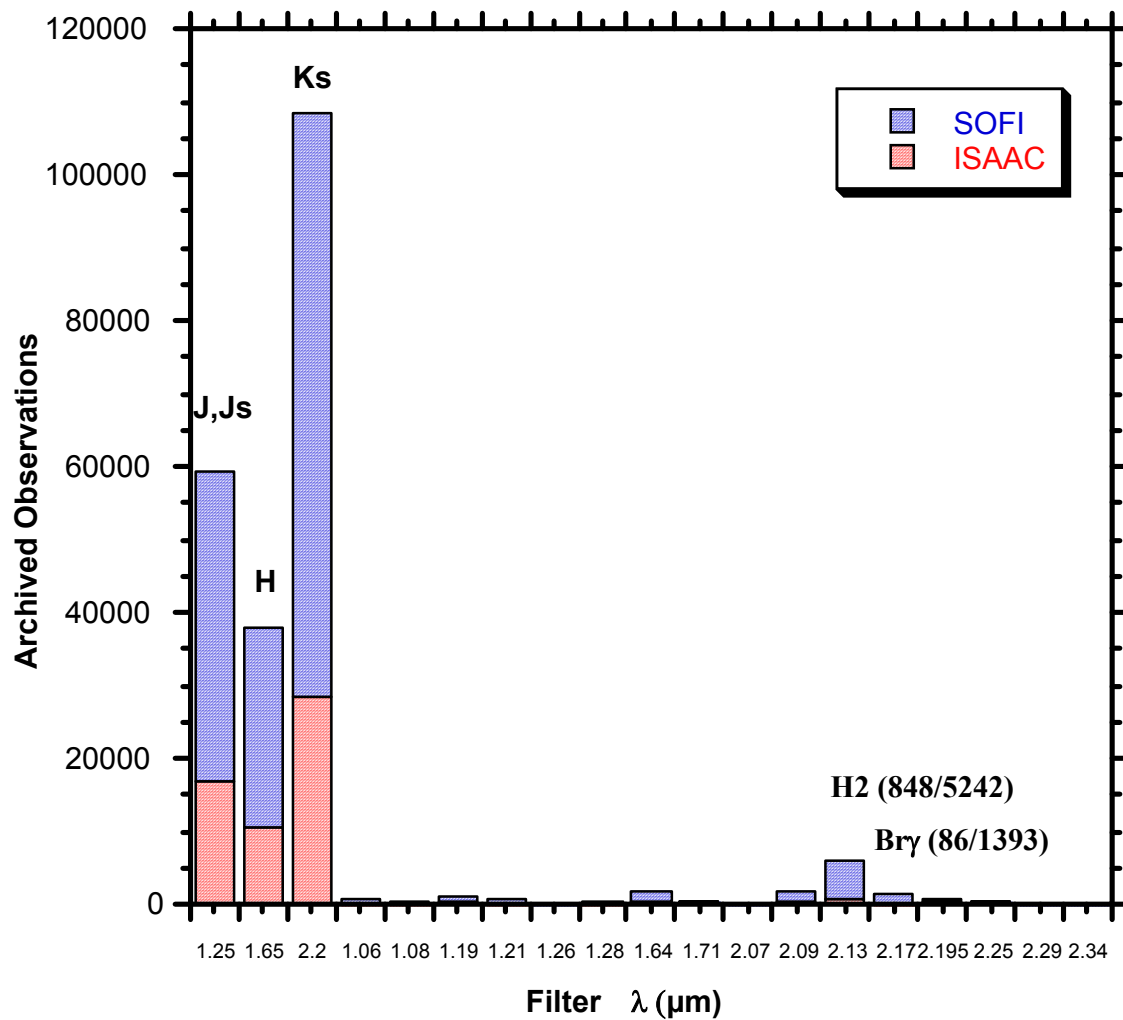
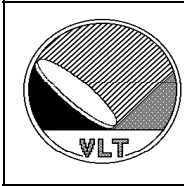


Fig. 2.2 Archived SOFI and ISAAC images through broad and narrow-band filters.

This demand reflects the now widespread importance of near infrared imaging in almost all fields of astronomy. Some of these programmes are for straightforward imaging for object identification, photometry to combine with other data etc i.e not necessarily demanding on telescope, instrument or observing conditions but nevertheless requiring a



Science case for 0.9-2.5 μ m infrared imaging with the VLT.
ESO /STC-323

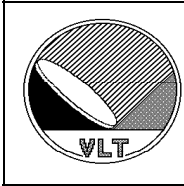


basic direct imaging capability. These and some of the 'wide field' surveys started with these instruments will probably transfer to VISTA in ~ 2007 . Of more interest perhaps are those programmes which require both the sensitivity and/or image quality achievable with an 8m class telescope operated under the best seeing conditions. Many of the ISAAC programmes to date in particular have featured these, including surveys for stellar discs, low mass stars, brown dwarves, free floating planets and high redshift galaxies. Not only have these programmes pushed to the VLT limit (e.g 30hr integrations/band under average 0.45" seeing in the FIRES programme), they have also demonstrated that the VLT is second to none amongst the current large telescopes for this type of work. Such programmes will also continue in the immediate future but are expected to become increasingly uncompetitive due to the aging of ISAAC and more specifically the fact that its 1kx1k arrays cannot be sensibly upgraded (because the field is limited by the instrument optics and mechanics) at a time when buttable 2kx2k arrays are already becoming available and should become the new workhorse detectors within a few years. The high priority placed on multi-object spectroscopy amongst the VLT 2nd generation instruments and the prospect of JWST are also likely to increase demand for imaging at the highest sensitivity for selecting interesting targets over the 5-10' field sizes of these instruments. Already, infrared cameras equipped with 2kx2k arrays or mosaics have or are about to be installed on 4m and 8m class telescopes (Tololo, KPNO, UKIRT, CFHT, Calar Alto, SUBARU, GEMINI ...). For HAWK-I we are proposing a 4kx4k contiguous mosaic of 2kx2k arrays with pixels of 0.125" and a field of 8.5x8.5' which is more than an order of magnitude larger than that of ISAAC and larger than any planned so far at the other 8-10m class telescopes.

3. The Basic Case for 0.9-2.5 μ m Imaging at the VLT

Both technologically and astrophysically the 'true' infrared starts around 2 μ m in the K band. Here the limiting noise begins to become dominated by shot noise on the thermal background of a warm telescope and measurements of the emission from the colder ($< 1000\text{K}$) Universe; highly obscured objects and the redshifted optical emission of galaxies at $z \sim 3$ become interesting or optimum (providing one can reach faint limits of $K > 22$ as demonstrated by the FIRES programme, see below). A camera like HAWK-I could maintain the VLT as the pre-eminent facility for such work because it produces images that equal or better any from other large ground based facility and would be the first camera with such a large detector array and hence field of this size on an 8m telescope. Until JWST is operational it would also outperform any of the Space Facilities because the new Hubble WFPC3 camera operates only at shorter (up to 1.7 μ m) and SIRTIF only at longer (3.6 μ m) wavelengths. In fact it is more likely that these space facilities will increase the pressure on ground based imaging as is e.g already the case with the VLT ISAAC contribution to the GOODS survey based on a SIRTIF Legacy Programme to study the CHANDRA deep field (Fosbury et al. 2001). It must not be forgotten, however, that HAWK-I would also be equipped with shorter wavelength broad and narrow band filters at wavelengths down to the Z band around 0.9 μ m.

Compared with existing cameras, the scientific gains of HAWK-I will derive from its capability for delivering well sampled images down to the best seeing limit on Paranal over a much larger field. As detailed below, this is of high scientific interest in many areas



Science case for 0.9-2.5 μ m infrared imaging with the VLT.
ESO /STC-323



from studies of the most distant galaxies to bodies within our own Solar System. Compared with ISAAC, HAWK-I will be nominally a factor ~ 12 faster for surveys down to the same magnitude limit. Compared to VISTA, planned for 2007 on Paranal, HAWK-I should reach about 1.5 mags. fainter on point sources in the same time or reach the same limit 16 times faster as well as providing up to a factor of 2 improvement in spatial resolution under the best seeing conditions. The VLT in service mode also offers the optimum chance of being able to exploit the best seeing conditions for those programmes which require them. Gains of this order can represent the difference between success and failure. In practice, the true gain is also much larger for many programmes which require not only the best seeing but also uniform photometry across the field. As stressed in some of the specific science cases, the effective time for producing a mosaiced image under the best seeing conditions may be many nights over several periods even if the required exposure time may only be minutes. Even then, seeing and depth may vary over the reconstructed field. Single shot programmes requiring the least time are certainly faster and more effective.

4. Selected Science Cases

4.1 Galaxy Evolution from Deep Multicolour Surveys

4.1.1 Scientific justification

The study of how galaxies formed and evolved is one of the major goals of present-day cosmology. The widely accepted “hierarchical” scenario predicts that galaxies form from smaller units that accrete gas and merge to build up present-day massive objects. Although the present version of the CDM models includes several free parameters, it is not as “tuneable” as commonly believed. All its parameters, indeed, are chosen in order to fit the properties of the local Universe and cannot be modified freely without worsening the local fits. For this reason, it is important to perform a detailed comparison between the model predictions and the observations directly at high redshift, where the physical processes that led to present-day galaxies are caught in the act. In this context, deep imaging surveys play a fundamental role, extending to fainter limits than the spectroscopic surveys.

A recent approach developed to access the earliest epochs of galaxy formation relies on deep multicolour surveys, where multiband images are taken with a complete set of standard broad-band filters in order to cover the overall spectrum of the galaxy and to discriminate the populations at different redshifts. Photometric redshifts are currently used for the bulk of the population. This technique allows to obtain an estimate of the galaxy redshifts with a typical uncertainty <0.1 that is accurate enough for many scientific applications.

The overall scenario that emerges from imaging and spectroscopic surveys is that most of the blue star forming galaxies that dominate the counts are low mass galaxies at intermediate ($z < 1$) redshift, and that the major epoch of formation of the more massive galaxies occurs at relatively larger redshifts. This implies that in order to study directly the processes that led to the formation of most massive galaxies we need to extend our observation to the bulk of the $z > 1.5$ galaxy population.



Science case for 0.9-2.5 μ m infrared imaging with the VLT.
ESO /STC-323



Compared to the optical bands, images in the NIR bands have the obvious advantage of sampling the rest-frame optical wavelengths for galaxies in the range $1.5 < z < 4$. This allows an easier and more accurate comparison between the properties of $z > 1.5$ and of local galaxies, minimizes the effect of dust extinction, and ensures that galaxies with no active or recent episodes of star formation are included in the census. In addition, the rest-frame optical spectrum is produced by the whole stellar population of the underlying galaxy, and therefore reflects its overall history, while the UV is produced mainly by the most massive stars and is therefore sensitive to its "instantaneous" properties.

This concept is emphasized in Fig. 4.1, where Bruzual and Charlot models are adopted to produce simulated spectra of galaxies at $z=3$ that look almost identical in the rest-frame UV, (redshifted into the optical bands at this z) but have quite different properties in the near-IR. In an extreme case, one spectrum is made from a young and actively star-forming galaxy with an overall stellar mass of $0.6 \times 10^9 M_{\odot}$, while at the other extreme a nearly-post-starburst galaxy with a larger age and a stellar mass content 30 times larger is shown to produce a much brighter K-band flux.

4.1.2 Recent studies with ISAAC and SOFI

Deep imaging with both SOFI and ISAAC have contributed substantially to cosmological studies during the last few years. Much of this has been done in Public Surveys such as EIS Deep, FIRES (HDFS + MS1054-03), GOODS (Chandra Deep Field), for which all data have been made public, plus a variety of individual programmes (K20, FORS deep field, selected high z clusters, narrowband surveys for emission line galaxies at $z \sim 2-3$ etc.).

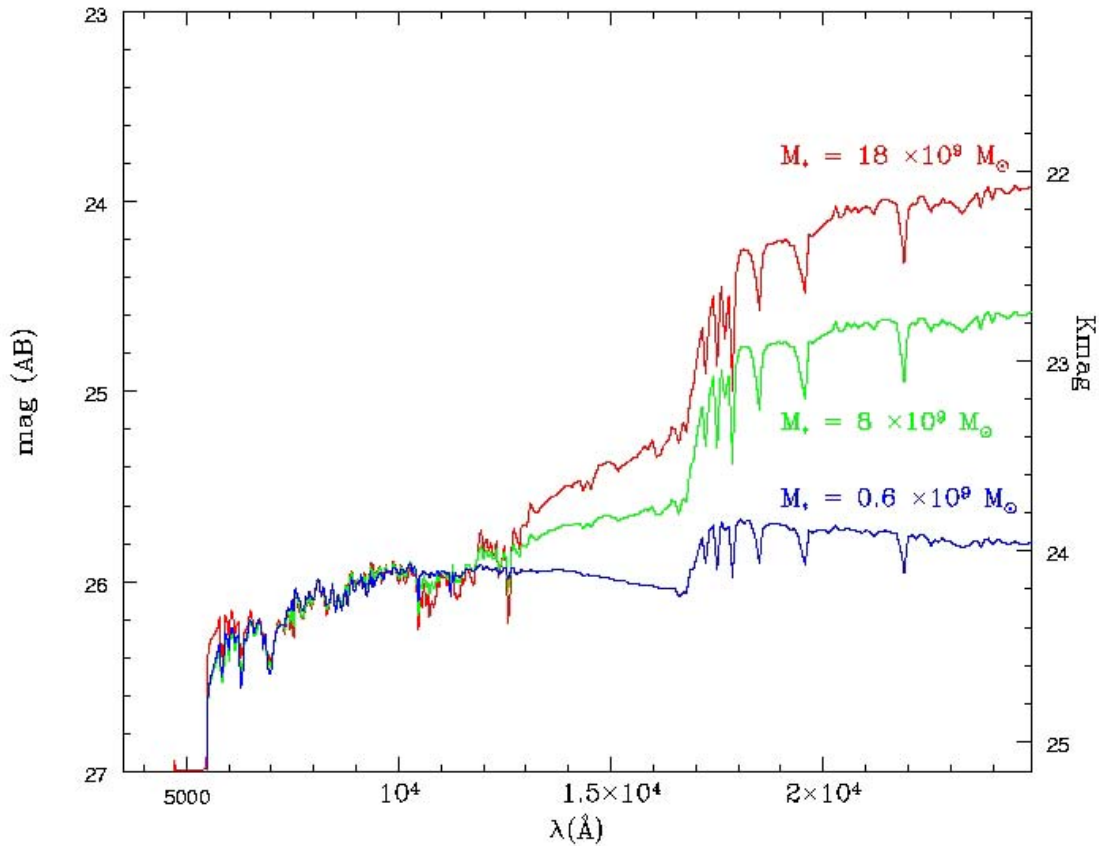


Fig. 4.1 Simulated spectra for galaxies at $z=3$ with different total stellar masses.

4.1.2.1. FIRES (Faint InfraRed Extragalactic Survey)

The deepest of the surveys to date is FIRES which was conducted with ISAAC under the leadership of Marijn Franx as PI and comprised observations in the Js, H and Ks bands of both the HDFS and a field centered on the $z = 0.83$ cluster MS1054 (Rudnick et al., 2001; Labbé et al., 2002; Franx et al., 2003; Daddi et al., 2003 and van Dokkum et al., 2003). The FIRES data are publicly available and have also been used scientifically by the group of Giallongo and others. For the HDFS, the ISAAC field of $2.5 \times 2.5'$ is well matched to that of WFPC2 on HST and thus only one pointing position was required/filter. Around 33 hrs of integration time was acquired under superb seeing conditions through each filter yielding a final image quality in the stacked data of $\sim 0.46''$ FWHM and magnitude detection limits (AB) of Js = 26.8 , H = 26.1 and Ks = 26.25. These are the deepest ground based limits reached to date and the deepest Ks band observations ever. Fig 4.2 shows examples of very red galaxies detected at $z \sim 3$ whose morphology is evident even at VLT resolution. A comparable total integration time of ~ 100 hrs and image quality of $\sim 0.45''$ were also achieved on the MS1054 field shown in Fig 4.3 but the area covered was $\sim 5 \times 5'$ i.e 4 positions/filter and the depth is thus correspondingly shallower

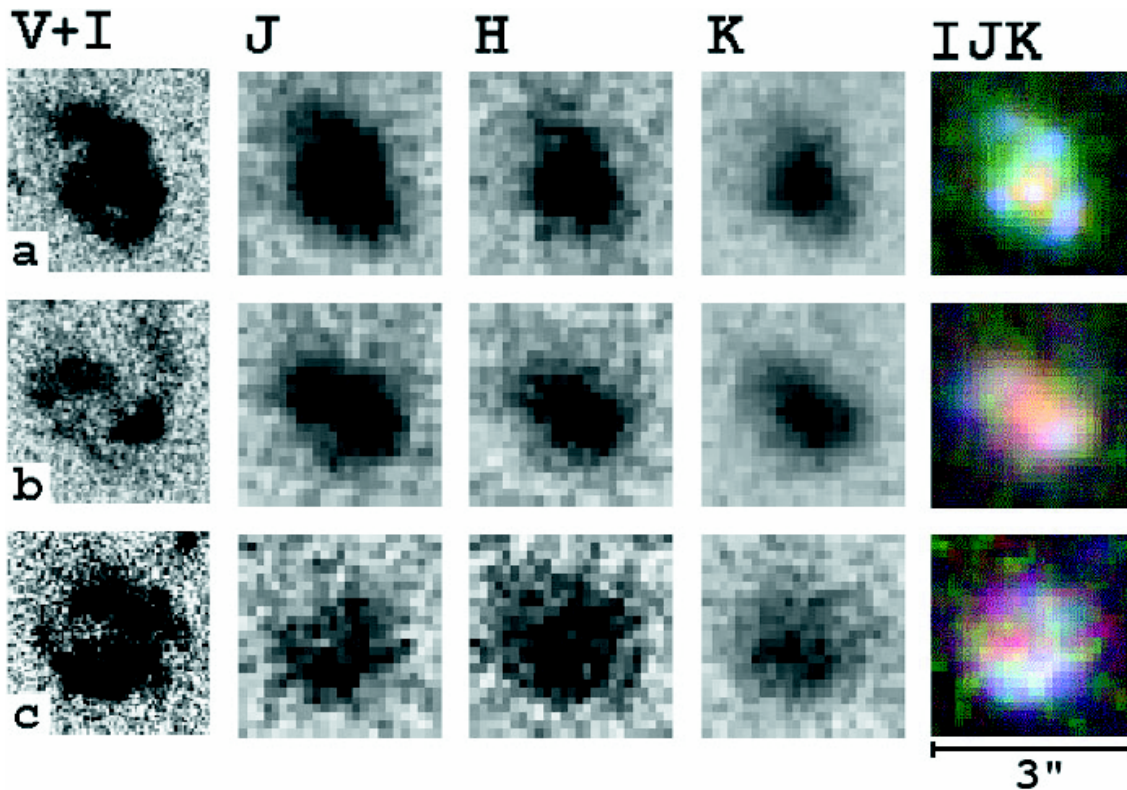
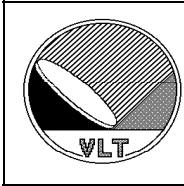


Fig. 4.2 Images of Lyman break galaxies in the HDF-S. Note that the K band (rest frame optical) FIRES images are more centrally concentrated than the WFPC2 V+I images.

Important lessons learned are that i) the VLT can indeed detect galaxies at $z > 3$ and that such galaxies, which are faint or undetectable in visible light, probably comprise $> 50\%$ of the stellar mass of the Universe at these redshifts ii) photometric redshifts obtained by combining visible and near IR photometry are now quite reliable iii) the image quality achievable is sufficient to study galaxy morphology at these high redshifts iv) clustering studies are both crucial and possible but limited by the small field sizes and v) cosmic variance is large e.g a new population of several tens of red galaxies at $z \sim 3$ discovered by the FIRES programme in HDF-S is absent in HDF-N.

The importance of depth is illustrated by Fig 4.4. which shows the photometric redshift distribution of galaxies in the HDF-S selected to different magnitude limits in the K band FIRES image. Down to $K = 21$, about 3 galaxies/arcmin² are detected at $z > 1.5$ and none at $z > 3$. Going 2 magnitudes deeper to $K=23$ the number density increases by a factor ~ 5 and galaxies begin to be detected at $z > 3$. This is largely expected since we are sampling the exponential tail of the luminosity function at these redshifts, and even modest gains in depth result in a large increase of statistics.

These galaxies are also of great significance in that their mass constitutes $> 50\%$ of the mass of the universe at these redshifts and more e.g than the, so far, better studied Lyman break galaxies detected by the U - dropout technique. The importance of image quality is illustrated by Fig.4.2 which shows that it is just possible from the ground to resolve the infrared morphology of these very red, high z galaxies. In fact some of these galaxies have been found to be very large in the infrared i.e rest-frame optical and to show profound



Science case for 0.9-2.5 μ m infrared imaging with the VLT.
ESO /STC-323



differences between their intrinsic optical and ultraviolet morphologies and are probably large, luminous spiral galaxies with a red bulge and patchy star formation in a diffuse disk. If so, this is a crucial finding in relation to CDM hierarchical models.

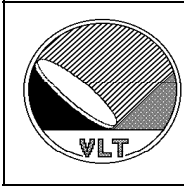


Fig. 4.3 I (WFPC2), Js,Ks (ISAAC) colour composite of the 5x5' MS1054 field observed in the FIRES programme.

4.1.4 Importance of Depth and Field

To progress with ground-based studies it is necessary to achieve the depth and spatial resolution demonstrated above but over much larger fields in order to accumulate statistically meaningful samples of high z galaxies and to follow up the study of clustering and cosmic variance.

The issue of field has already been highlighted by the GOODS programme which is requiring 32 ISAAC positions/filter to cover the Chandra/SIRTf field i.e a penalty of nearly 2 mag. (or a need to spend about 3200 hrs of the best seeing condition observations



Science case for 0.9-2.5 μ m infrared imaging with the VLT.
ESO /STC-323



to match the sensitivity of the FIRES survey of HDFs). Other relatively large and at the same time deep multicolour surveys in the optical bands are foreseen with the ACS/HST camera (treasury programs of about 1.5x1.5 deg have been submitted for cycle 12) and for other wide field imagers at 8m class telescopes (e.g. VIMOS at the VLT, Suprimecam at Subaru and LBC@LBT where the Italian and German communities will be involved). All these optical surveys need deep NIR coverage with good spatial sampling (to optimize the matching with faint galaxies showing often blended features as seen from HST) and extended over areas of the order of a square degree. This requires e.g. 36 frames per band if the FoV is of the order of 10x10 arcmin² implying a still reasonable amount of total exposure time (e.g. 216h) for a single exposure time per field of e.g. 6h in the K band. Although wider NIR fields are foreseen at 4m class telescopes, the need for accurate (s/n>5 and about 0.15"/pix) photometry down to K=23 is mandatory to sample in the near IR galaxies as faint as I=26-27. For this reason, a relatively wide imager at an 8m class telescope like VLT can allow European astronomers to investigate the physical properties of galaxies at the very high redshifts $z=5-10$ or higher where the processes of star formation and reionization of the Universe are believed to occur. In the following, a few examples are presented to emphasize the importance of such an instrument for observational cosmology.

4.1.5 Some specific HAWK-I galaxy evolution programmes.

4.1.5.1 The B-band luminosity function from $z=0$ to $z=4$

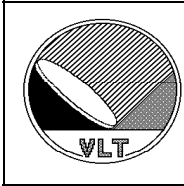
The availability of a large sample of galaxies from $z=0$ to $z=4$ with continuous sampling from the (observed) B to the K bands would allow us to draw the self-consistent evolution of the rest-frame B - band luminosity function, that is one of the main statistical descriptions that are used to study galaxy evolution. Preliminary results in the Hubble Deep Field South show that a pronounced brightening appears at high redshifts in the interval $z=2.5-3.5$ with respect to the local LF (Fig. 4.5). This excess could mark the epoch where major episodic starburst activity is present in the galaxy evolution. Merging events between galaxies in common halos are frequent at these high z and could be responsible for the measured activity. However this preliminary analysis is based on only 70 galaxies with $K<23$ in the HDFs/N, so it is clear that both deep and wide NIR surveys are needed to study the high z blue LF for different galaxy spectral types (see below).

4.1.5.2 The detection of passively evolving (quiescent) galaxies at $z>2$

CDM models predict that galaxies form through a nearly continuous history of accretion and consequent star-formation: the search for quiescent galaxies at large redshifts (i.e. observed only in the near-IR) is therefore a critical test for these models, and can provide clues to the origin of present-day ellipticals.

4.1.5.3 Searches for extremely high redshift galaxies.

Searches for $z>6$ objects via the dropout technique are already underway at the VLT with ISAAC, although the small field of view of this instrument makes wide-area surveys prohibitively expensive in terms of observing time. For this reason current projects have more the size of "pilot studies" rather than of conclusive surveys. Yet, the push to identify objects at higher and higher redshift is expected to remain strong in the future. Actually, after WMAP favouring re-ionization at $z>10$, one may expect a boom in the number of



attempts to detect a population of near-IR dropouts (z-band, J-band, or even H-band dropouts). The factor ~ 10 increase in field over ISAAC would make HAWK-I very attractive for these kinds of searches, offering to the ESO community the possibility to identify fairly large samples of extremely high-z candidates, perhaps just a couple of years before JWST may be able to obtain their spectra. Such very high redshift objects are expected to be rather strongly clustered, hence surveys over large areas are essential to avoid being dominated by cosmic variance. On the other hand, these near-IR dropouts will be quite faint ($K^* \sim 24 - 25$ AB at $z \sim 6$ cf. FIRES limit of $K \sim 26.3$) and compact, making HAWK-I more efficient than e.g. VISTA, thanks to the combination of the VLT's larger collecting area and HAWK-I's better sampling of the PSF.

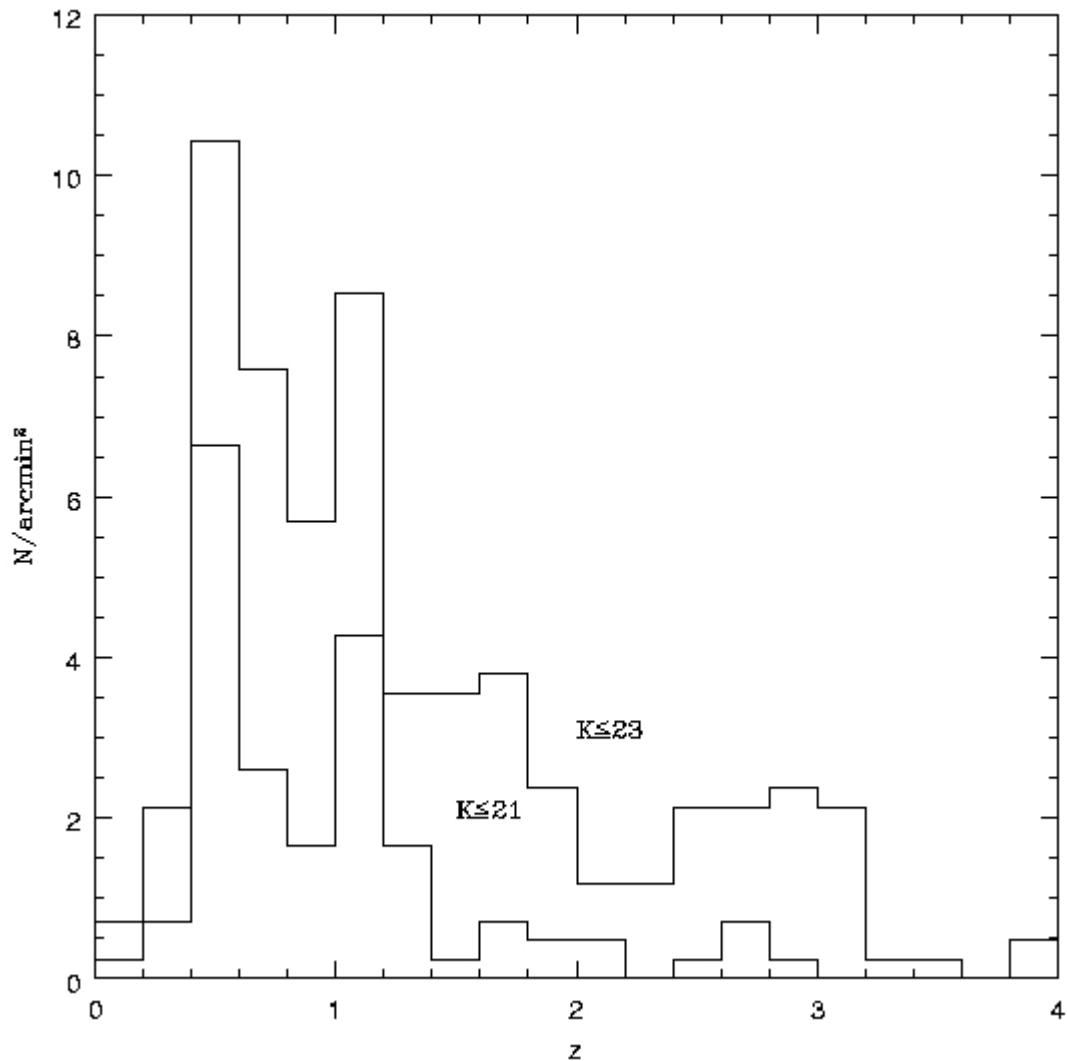
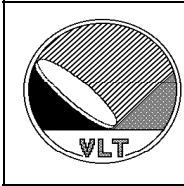


Fig. 4.4 Photometric redshift distribution in the WFPC2 HDFs field from the FIRES survey.

4.1.5.4 Structural properties and morphological evolution at intermediate and high z

The main morphological parameters can be measured not only from space but also from ground based images with good seeing and sampling: the availability of large samples of



galaxies observed in the rest - frame B band can allow to trace for the first time the morphological evolution of galaxies from $z=0$ to $z=4$.

While the study of galaxy evolution has often focussed on integrated light properties in the past, there is an ever increasing interest in understanding the origin of the Hubble sequence: How do bulges and disks form? What exactly are the evolutionary stages, what role is played by morphological transformations through interactions and mergers? And what are the properties of galaxies hosting nuclear activity during parts of their evolution?

High-resolution imaging has a key function in this research area. HST has probably brought the biggest advance, and will continue to do so with the major imaging surveys conducted by ACS. Nevertheless, HST capabilities are fundamentally limited in two aspects: (1) the small telescope size impedes going to very low levels of surface brightness. (2) There is no near-infrared facility matching the capabilities of ACS. Note that the field of view of NICMOS is an order of magnitude too small to be efficient except when targeting single objects.

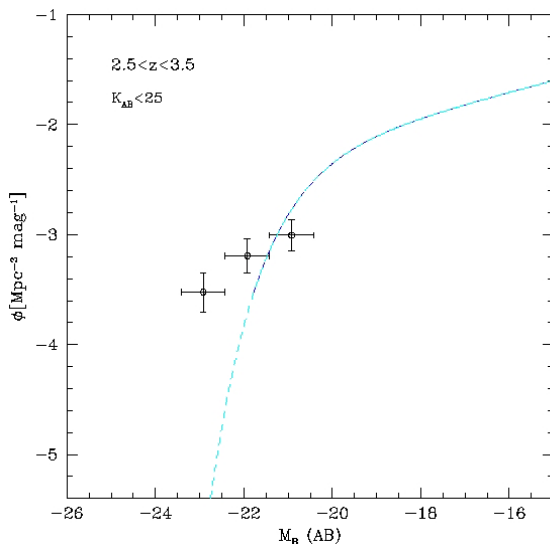
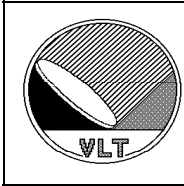


Fig. 4.5 Rest-frame blue luminosity function for galaxies in the HDF5-N at $z=3$. The continuous curve is the Schechter fit to the local LF from the Sloan survey

Yet the NIR domain holds vital astrophysical information about galaxies especially at higher redshifts. High-resolution NIR imaging is therefore still largely a task for ground-based telescopes, of course requiring excellent seeing. But even today the situation at ESO is less than optimal. The field of view of ISAAC is considerably less than that of a single ACS pointing, making any major follow-up extremely expensive in terms of observing time. A similar point can be made about NIR complements to VIMOS surveys, driving for structural properties of redshift-resolved samples.

The proposed HAWK-I instrument would provide a large improvement for this type of work because it will provide the sensitivity and well sampled images required for seeing morphological detail but over a field significantly larger than that of ISAAC and sufficient to begin surveys of statistically significant samples. As an example, the ongoing survey of the extended Chandra Deep Field South with the ACS on HST (GEMS) will yield more than 10000 galaxies for spectroscopic follow-up within a contiguous area of $30 \times 30'$.



4.1.5.5 Estimate of the cosmological mass density as a function of redshift

This becomes possible because the stellar mass content in high z galaxies can be obtained from their rest-frame optical luminosities measured in the near infrared.

4.1.5.6 The Cosmological Clustering of the Stellar Mass.

The clustering of galaxies and its evolution have now been estimated up to $z=4$ either with spectroscopic or photometric redshifts. The main limitations in the interpretation of these data are cosmic variance and the uncertain relation between the luminosity and mass of the galaxies. Widely different cosmological scenarios can be reconciled with the observations due to the complex interplay between the clustering of mass and the variation of the effective bias of the galaxies. This degeneracy can be broken only with an estimate of the typical mass of the structures that is available through IR observations.

In hierarchical models, enhanced clustering of galaxies with respect to the underlying matter distribution is expected at high redshift, as a result of the so called biased galaxy formation scenarios. At $z>2$ only populations with active star-formation have been selected in significant numbers during the previous decade and their clustering has proved to be large, in broad agreement with models.

The FIRES survey has shown for the first time that near-IR selected galaxies at $z>2$ appear even significantly more clustered than optically selected galaxies (like Lyman Break Galaxies) at the same redshift. In particular, as shown in Fig. 4.6 the clustering level appears to correlate strongly with the near-IR colours (i.e. J-K) of galaxies at $2<z<4$. The most likely explanation of this effect is that the redder J-K colours may be due to older stellar populations.

These results were made uniquely possible by the ultra-deep near-IR imaging, obtained for the first time in the FIRES survey and they appear to open new science opportunities for the study of the clustering of evolved populations at $z>2$.

These galaxies possibly correspond to the remnants of the first generation of star-forming galaxies that were active at much larger redshifts $z\sim 4-6$, and will evolve into extremely red objects at $z=1$ and massive early type galaxies in the local universe.

However, despite the very long integrations of the FIRES project, the measured correlation lengths are only slightly more than significant, with signal to noise ratios around 4 obtained by adding together all populations of $2<z<4$ K-selected galaxies and with crude median splitting of the high redshift sample with J-K colour. The main limitations are obviously the small number of galaxies detected (a few hundreds) and the small area covered by FIRES which makes it highly sensitive to cosmic variance effects. In fact, the population of red, high z galaxies detected by FIRES in HDFN does not exist in HDFN.

To make progress, as much longer integration times with ISAAC are practically infeasible, new instruments with a larger field of view at 8-10 m class telescopes would be needed. HAWK-I appears to be a very valuable instrument to investigate the clustering of evolved galaxies at $z>2$. For example, assuming FIRES-like depth to be obtained over a 8×8 arcmin² field, it would allow to assemble a 10 times larger sample of galaxies thanks to its larger field. This will lead to a reduction in the measured error on the two-point correlation functions by a factor of 3, thus correspondingly increasing the S/N ratio by a



similar factor if the FIRES strong levels of clustering are confirmed. At the same time, the enhanced signal will allow investigation of the dependence of clustering in more detail as a function of redshift (e.g. binning in several redshift bins at $z > 2$) and/or as a function of colours and galaxy properties. Investigations of the angular separation dependence of the angular clustering would also be made possible, allowing to discriminate contributions to the clustering due to the multiplicity with which halos are populated at high redshifts (halo occupation term) from those arising from the genuine halo-halo clustering (the bias term).

4.1.5.7 High z galaxy clusters

Near infrared imaging/photometry is becoming routine and is essential for the study of high redshift clusters starting with their basic identification and photometric redshift estimates.

Deep near infrared images are required, for example, to measure the rest frame red sequence needed for fundamental plane studies as well as being important for deriving stellar masses for all the cluster galaxies. In the best seeing conditions, one can study the morphological (i.e. B/T) properties vs. colours for the brightest galaxies. Wide fields at these depths with good image quality are important to characterize the population on the outskirts of the cluster as well as the field population which will presumably fall into the cluster in the future. Because there is significant evidence that galaxies falling into clusters may be preprocessed by the small overdensities (i.e. groups) in which they reside before falling in, characterizing the environments on the outskirts of the cluster is quite important in nailing down the infall history and the effect of environment on SFH, colour, and morphology.

Over the past decade, rich galaxy clusters have been used to measure cosmological parameters, to trace large scale structure, to study the evolution of galaxies in rich environments and, more recently, to study galaxies at very high redshifts through the amplification of background sources via gravitational lensing (see below).

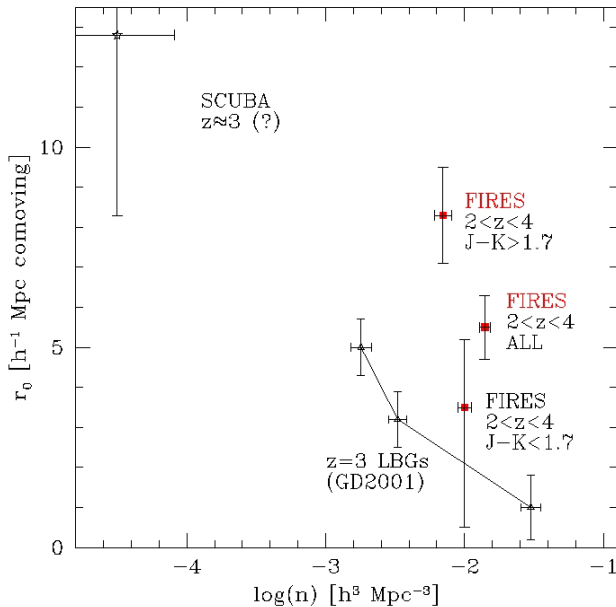


Fig. 4.6 Co-moving correlation lengths for FIRES galaxies at $2 < z < 4$, LBGs and SCUBA galaxies as a function of number density. Note the increase as a function of colour for the FIRES galaxies.

Galaxy clusters form from the gravitational collapse of large fluctuations in the primordial density field. The number of clusters and the evolution of the space density of clusters is a sensitive function of the cosmological parameters (White et al., 1993). Present studies have measured the RMS of density fluctuations at $8h^{-1}$ Mpc scales (σ_8) and the matter energy density (Ω_M). These results are consistent with those provided from studies of the Cosmic Microwave Background, the luminosity distance relation of type Ia SNe and studies from large galaxy redshift surveys (Rosati et al, 2002).

A Ks-band image of CL1252.9-2927 detected by ROSAT and one of the most distant, spectroscopically-confirmed galaxy clusters is shown in figure 4.7. At a redshift of 1.23, this cluster was observed at a time when the universe was 40% of its present age. The image is 3.5' on a side and is made up of a mosaic of four ISAAC fields. One ISAAC field covers 2.5' on a side. The total integration time for the Mosaic is 24 hours, or six hours for each tile. Although the central part of the cluster fits nicely into the FOV of ISAAC, some of the galaxies near the edge of this field are also confirmed cluster members. Rich clusters have a typical diameter of 1Mpc, which projects to 2 arc minutes on this image. However, clusters form from regions that are several times larger. Current n-body simulations show that clusters form at the intersections of large unbound structures such as filaments or super-clusters. As we start to find clusters at redshifts between 1 and 2, which is where one expects most of the clusters to be forming, we will want to study the cluster formation process in detail and this means that we will want to study regions which are of the order of 5 Mpc in size. For redshifts between 1 and 2, this spans 10' on the sky. Observing such a region with ISAAC to the depth that is required is clearly not feasible. It would be feasible with HAWK-I.

Although the number of confirmed clusters at redshifts beyond $z=1$ has increased from none to only several spectroscopically confirmed candidates over the past few years,



serendipitous X-ray surveys with XMM-Newton and AXAF-Chandra and dedicated mm surveys surveys will increase this number by an order of magnitude. In particular, future mm surveys, which detect clusters via the SZ effect, have the potential of providing a redshift-independent, mass-limited survey of several 10s of clusters per square degree up to redshifts of two. Such a survey will not only place tight limits on Ω_M , Ω_Λ and σ_8 , but may even also place limits on the equation of state of the dark energy (Carlstrom et al. 2002).

Both current and future X-ray and mm surveys will need IR imaging to confirm clusters that have redshifts greater than one. Given the likely size of these surveys (10s of square degrees) and given the likely number of clusters per square degree (several 10s), a wide-field IR survey that covers exactly the same area will be an efficient way of confirming these clusters and studying large scale structure at an epoch when clusters are forming.

With regard to depth, limits of $J=23$ and $K=21$ are needed to detect an an L^* galaxy at $z=1.25$. The two giant ellipticals in the centre of the cluster shown in Fig. 4.7 are 3.5 magnitudes brighter than L^* . To reach $z=2$ one needs to go about a magnitude fainter.

It takes about 10 minutes in each filter to reach $J=23$ or $K=21$ with ISAAC. To cover 1 square degree, approximately 800 ISAAC fields would be needed and this would take about 400 hours of telescope time. HAWK-I would cover the same area with approximately the same depth and image quality in 45 hours.

To summarize, HAWK-I will allow one:

- i) to image the same area as that covered in future high redshift cluster surveys that will be conducted at X-ray and mm wavelengths,
- ii) to study the environment of high redshifts clusters to understand better the processes involved in their formation.

4.1.5.8 Gravitational lensing by galaxy clusters

a) Strong lensing

Clusters of galaxies at redshifts between 0.1 and 0.5 are currently recognized as efficient gravitational lenses that distort the galaxies in their background, eventually giving multiple arc systems. Only a few per cent of magnified arclets have been reported so far with a redshift larger than 1.5 because their magnitude is usually beyond the detection threshold of ground - based telescope due to the cosmological dimming of their surface brightness and luminosity. The number of distant sources within the focal plane of the lenses is high (Blandford 2001, "The Future of Gravitational Optics" astro-ph/0110392) but their detection needs deep observations on 8 meter class telescopes - especially in K band. As an example, a few clusters like A370, MS2137 have been successfully observed during the last 5 years with SOFI, on a four meter class telescope, and with ISAAC on the VLT. In each case, it was proven that we can detect a few new gravitationally magnified sources in their field thanks to the VLT IR imager. Four hours exposure time in K allows the detection of new objects with a magnitude $K=22.5$. In Fig 4.8 below we give an example of an R drop out object in the field of MS2137-23 that looks like a luminous elliptical galaxy at $z > 4$.

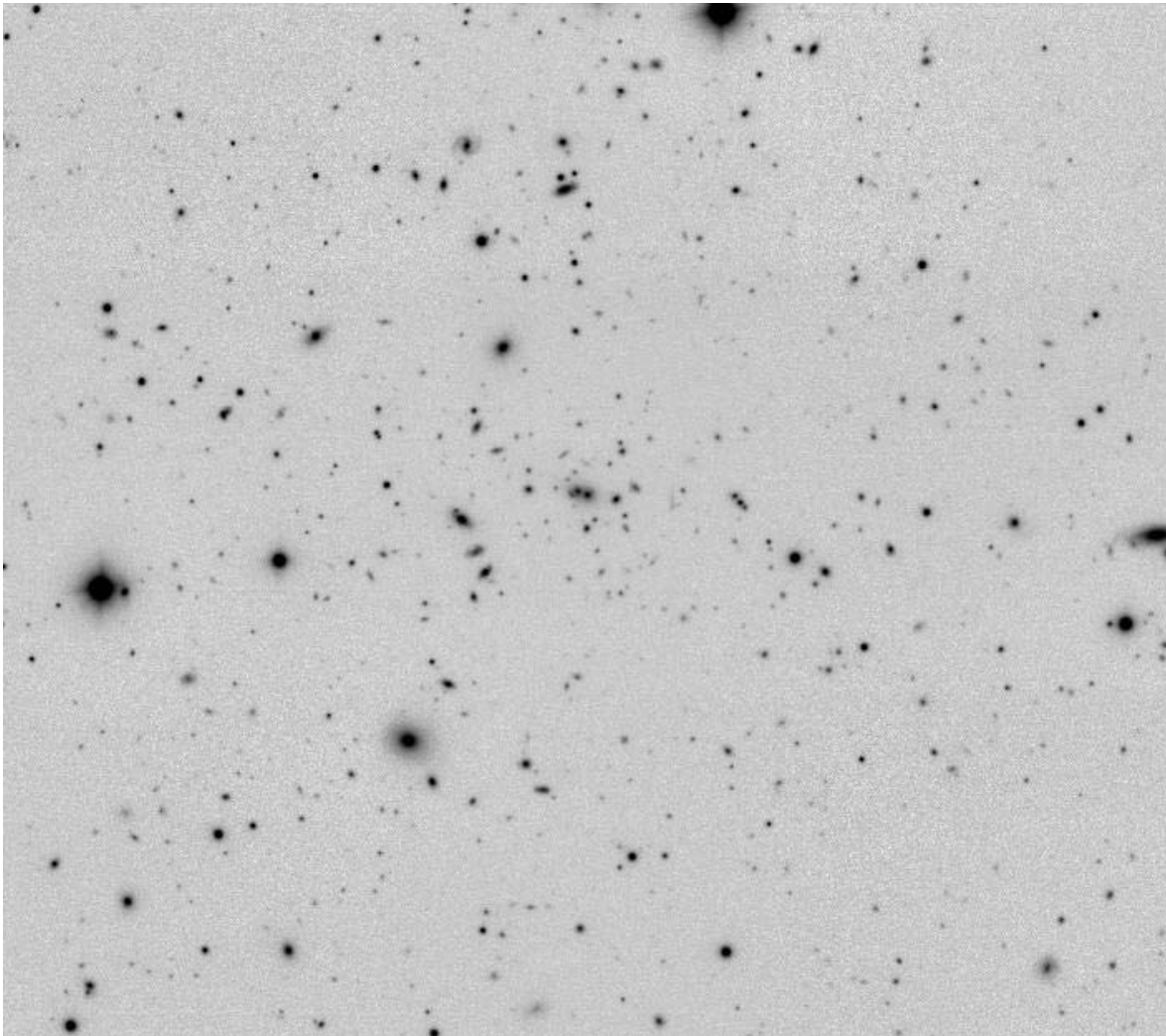


Fig. 4.7 Ks band mosaic of ISAAC images of Cl1252.9-2927, one of the most distant, confirmed, galaxy clusters at $z = 1.23$.

Deep IR observations of cluster lenses also led to the discovery of a new class of highly magnified object at the largest redshift $z > 6$ (Hu et al 2002). These events result from the galaxy lensing effect of a cluster member which is strongly enhanced by the natural convergence of the cluster (additional mass sheet). The Einstein radius of cluster members is significantly increased and the number of such extra magnified distant objects in a cluster field of about 5 arcminutes is 2 ± 1 for arc clusters at $K=22.5$. These IR sources are often almost merging within the bluer deflector but can be easily detected on (V-K) images as shown in Fig. 4.9. Occasionally, they can take the shape of an optical ring. Finding these distant objects is of great interest for future mm survey of galaxies and to study the star forming rate as a function of cosmic time.

The survey of highly magnified IR objects in the field or cluster field will be one of the best ways to detect extremely distant galaxies at $z = 6-8$ or more. One can predict that I-Z drop-outs could be found quickly if a deep IR cluster survey is implemented on the VLT.

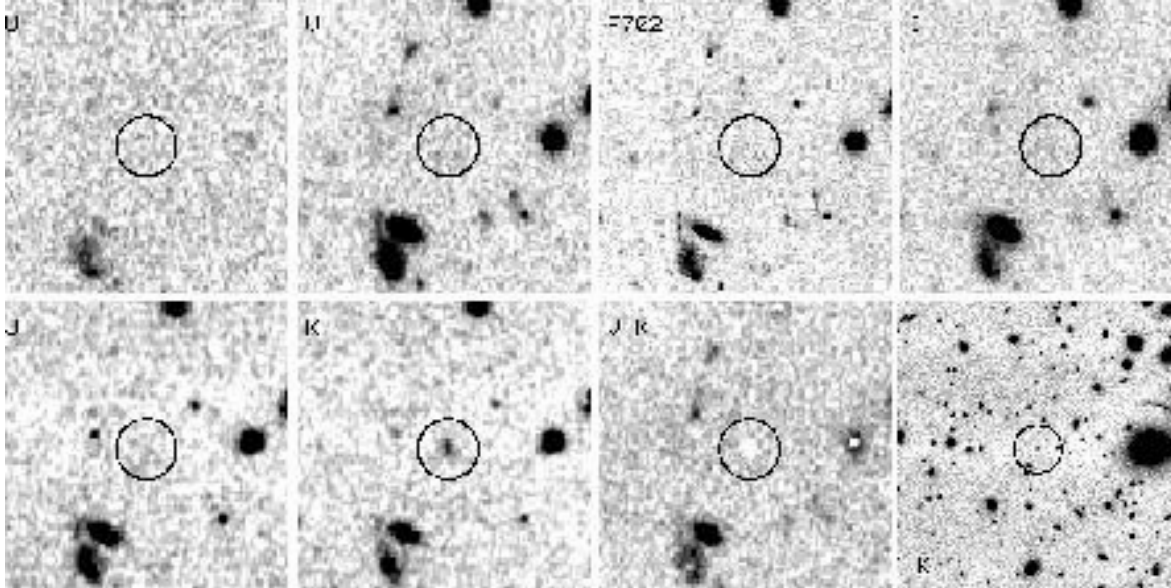
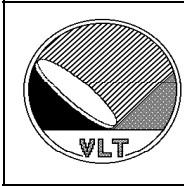


Fig. 4.8 A newly discovered IR arclet in the field of MS2137-23 (FORS/ISAAC images). Note the clear orthoradial elongation and the SED drop-out in the optical bands.

b) Weak lensing

A typical scale length of the weak lensing effect that can be used to reconstruct the mass distribution of a galaxy cluster is about 5-8 arcminutes (Mellier Y.,1999). This is approximately the field size of FORS 1 and FORS2. Of great importance is the possibility to determine the colour redshift of the background galaxies which are radially distorted by the gravity field of cluster lenses. So far, mass reconstructions just consider that all the background sources are located at an average redshift of about 0.8. However, for a cluster say at $z=0.3-0.4$ the apparent distortion of a background galaxy varies quite rapidly with the angular distance ratio D_{ol}/D_{os} when the source redshift is moved from 0.5 to 1. It results in a redshift noise in the mass reconstruction that is dominant on spatial scales larger than an arcminute, a limitation when trying to probe the exact variation of the potential slope at large radius (below one arcminute the number density of galaxies, typically 20 galaxies/arcminute square for a WL analysis becomes the main source of error).

The only way to measure accurate colour redshifts is to cover a large spectral range from U,B,V,R,I,Z to J,H,K deep imaging on the same cluster field. In such a case, it becomes possible to reconstruct the mass profile of clusters up to several arcminutes from the center and to couple this mass reconstruction with a strong lensing analysis (Gavazzi R. et al 2003). Such studies can be pushed up to 3D reconstructions of the mass distribution of Dark Matter, X-ray gas and stars with the ultimate goal of really understanding the dynamical processes that link the various mass components and to compare the observational results with numerical simulations. Challenges are to validate the existence of cuspy models "a la" Navarro, Franck and White, determination of concentration



parameter and slope departure from SIS models and to observe the triaxiality of DM halos predicted by the CDM cosmology.

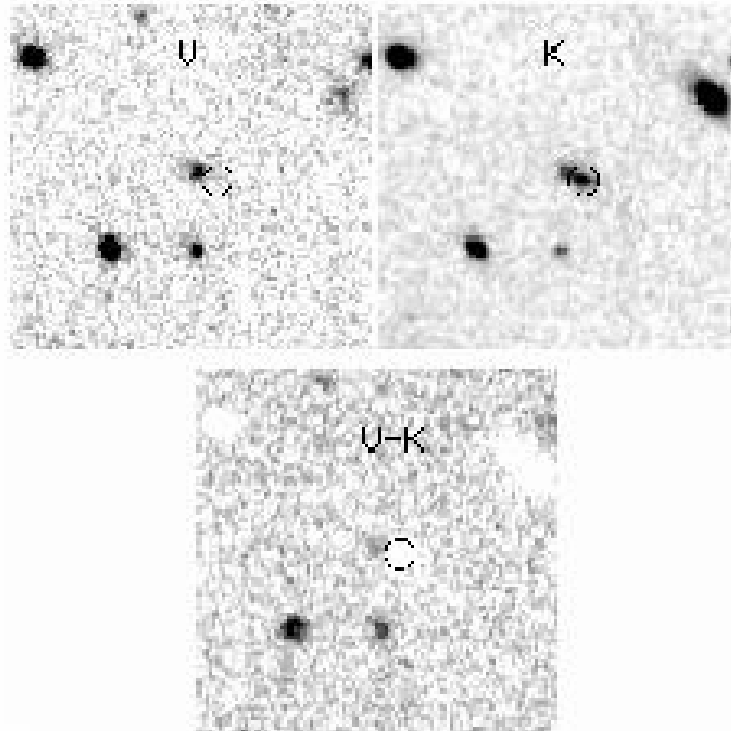


Fig. 4.9 Example of a highly magnified IR object (K=20.5) by a close cluster member in the field of MS2137 (tentative colour redshift $z=5.4$).

In conclusion, the availability of a deep IR imager that exactly matches the FORS field will be crucial for all the cluster lensing studies. It will strongly improve the lens modelling and dark matter mapping with a better knowledge of the colour redshift of background galaxies. Besides, it is easily guessed that this is one of the best ways to search for the most distant galaxies observable in the Universe with the I-Z drop out technique.

4.1.5.9 Searches for emission line galaxies at $z\sim 2-3$.

Several surveys have already demonstrated the possibility of detecting H_α [OIII] galaxies at $z\sim 2-3$ by means of deep narrow-band imaging in the near infrared. Based on such a survey with SOFI at the NTT, some 5 galaxies were discovered in this way within the deepest field of ~ 20 sq. arcmin obtained with a total integration time of ~ 6 hrs. Follow-up spectroscopy with ISAAC was needed to establish that these are [OIII](4959,5007) emitters at $z = 3.2$ (Moorwood et al. 2000; 2003). Extrapolating to HAWK-I implies that one could find ~ 15 galaxies per field in ~ 1 hr exposures which would match well the multi-object spectroscopy follow-up capabilities of KMOS.



Science case for 0.9-2.5 μ m infrared imaging with the VLT.
ESO /STC-323



This technique has also been used to study extended gas and members of galaxy clusters centred on high z radio galaxies by means of their H α emission (Kurk et al., 2002).

4.1.5.10 Star formation rate density at $z=0.5-3$

Emission line surveys by imaging in narrow-band filters as described in 4.1.5.9 plus follow-up spectroscopy of candidate detections provides an efficient means of determining H α luminosity functions and hence star formation rate densities in well defined comoving volumes at a known redshift.

4.2 Multi-wavelength Observations of Normal and Active Galaxies

4.2.1 Stellar content of nearby galaxies

Combining optical and near infrared imaging of nearby galaxies of all types has become routine and is yielding important information on their stellar content. Examples are the pioneering discovery of young stellar clusters in the 'old' elliptical galaxy NGC 4365 based on HST and ISAAC images (PR 11/02) and various results from FORS/ISAAC imaging of the halo of NGC 5128 (Centaurus A) in which individual stars could be resolved (Rejkuba et al., 2001). Future developments of this technique will clearly require high sensitivity and the best possible spatial resolution over fields of several arcmin.

4.2.2 Obscured AGN and evolution of the accretion in the Universe

A significant fraction of the radiative energy density in the Universe is due to accretion of matter onto super massive black holes in galactic nuclei. Most of this radiation, emitted in the optical, UV and soft X-ray bands, cannot be directly observed because it is absorbed by circum-nuclear matter and reprocessed and re-emitted at longer wavelengths (the bulk of the accretion power is therefore detectable above about 2 keV and in the infrared). Conversely, most of the information available today on AGN evolution comes from optical-UV surveys. A large fraction of the accretion power could have been missed by these surveys. To study the evolution of the accretion in the Universe, and to obtain reliable estimates of the super massive black hole number density at high redshift, it is imperative to perform sensitive multiwavelength surveys, from hard X-rays to infrared wavelengths.

One of the most interesting results of recent Chandra and XMM surveys is the discovery that about 20% of the hard X-ray sources have very faint optical counterparts ($R \geq 25$) and X-ray to optical ratios 10 times higher or more than that typical of broad line AGN. Near infrared follow-up of the CDFN and of the HELLAS2XMM survey of high X-ray to optical ratio sources show that many of them have relatively bright K band counterparts, with $R-K \geq 5-7$, typical of EROs. These extreme X-ray sources could be distant, $z=2-5$, highly obscured quasars, i.e. quasar 2. If this is the case they may carry the largest fraction of accretion power from that shell of Universe, a fraction largely missed before.

The picture that is starting to emerge from both observational data and theories of galaxy and AGN evolution is intriguing. Luminous AGNs may follow the evolution of spheroids. Powerful AGNs may help in inhibiting star-formation in these galaxies, which therefore would have red colours. On the other hand, lower luminosity AGNs could be associated with galaxies in which the star-formation is on-going, and share a similar evolution. However, a comprehensive and quantitative description of the onset of accretion powered



sources and its connection with galaxy formation and evolution is still far away. Many questions remain open or to be quantitatively verified by further analyses.

At a 2-10 keV flux limit of 10^{-15} erg s $^{-1}$ cm $^{-2}$, reachable by Chandra and XMM with deep exposures, there are between 400 and 700 highly obscured AGN per square degree, i.e. 7-12 per HAWK-I field of 8.5'x8.5'. As mentioned before most of these sources have $R \geq 25$ and are therefore inaccessible to optical spectroscopy even with 10m class telescopes. Conversely, the majority of these sources should have $K=21-23.5$ and should therefore be accessible to deep HAWK-I exposures. The only means to assess the redshift of these objects is through the comparison of their optical-NIR photometric SEDs to galaxy and AGN templates. Thanks to its sensitivity and wide field HAWK-I may provide key pieces of information to derive reliable photometric redshifts for a sample of highly obscured X-ray sources large enough (several hundreds) to determine their luminosity function and its evolution on several luminosity dex and up to $z=4-5$. This is crucial to verify whether the evolution of highly obscured AGN is similar to that of the much better studied broad line AGN (as assumed in AGN unification schemes and models of the X-ray Cosmic background).

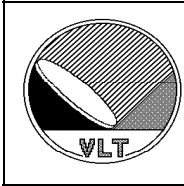
The use of a wide field NIR imager will provide a very important synergy for the large European community using multiwavelength facilities. In particular, XMM fields are providing a huge database of X-ray targets that will require some optical-NIR follow up. Each 30 arcmin XMM field could contain about 100 faint sources in addition to the main target, for typical exposures of 50 ksec. This "serendipitous" survey will cover about 100 square degrees per year. The XMM Survey Science Centre is funded to produce a homogeneous database which will be of great importance for the next years. A NIR imager at the VLT with a field of the order of 10x10 arcmin 2 could provide an adequate coverage to any XMM or Chandra field. Given the possibility that a significant number of sources are obscured galaxies and quasars, IR colours reaching $K=22-23$ are particularly valuable to characterize his population.

A second example of multiwavelength application comes from the NASA Space Infrared Telescope facility (SIRTF) that will be important to explore the evolution of normal and active galaxies. In particular large shallow surveys like SWIRE, in which the European community is involved, will cover selected regions of the sky in 7 bands from 3.6 to 160 μ m over 70 sq. degrees. In this respect, HAWK-I could provide the NIR complement in selected areas where optical imaging is also available to characterize the spectral energy distribution of far infrared selected objects.

Yet another application is the observation of SCUBA/APEX/ALMA sources at high redshift. Locating the counterparts to SCUBA sources has so far proved to be extremely difficult and once they have been identified, high quality NIR images are necessary to determine their morphology, especially since they are often almost invisible in the optical.

4.3 Structure and Evolution of Nearby Galaxies

The global quantities and the internal structure of disk galaxies are essential properties for the understanding of the evolution of such systems. Three main points in this context are a) the detailed characterization of global properties including morphology to establish a reference for a comparison with galaxy populations at higher redshifts. b) the internal structure of the disks to understand different types of perturbations (e.g. bars and spiral



Science case for 0.9-2.5 μ m infrared imaging with the VLT.
ESO /STC-323



patterns) and their ability to transfer angular momentum and mass, and c) the relation between star formation and other global properties.

4.3.1 Global properties

Detection of possible evolution of the global properties of disk galaxies as a function of redshift requires a local reference sample. One such property is the mass distribution of disks which can be estimated from near-infrared maps.

4.3.2 Internal structure

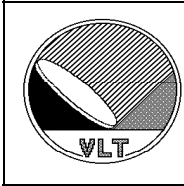
Secular evolution of galaxies due to density waves in the disks of galaxies may redistribute both mass and angular momentum. They may further introduce shocks in the gas and thereby stimulate star formation and gas flows toward the center. The morphology of such waves is best studied in the near-infrared bands which mainly show the old stellar disk population and are little effected by dust. Such maps can be used to estimate the potential perturbations associated with bars and spiral arms. Although this can be done currently for the inner parts of galaxies, it is very difficult to study perturbations in the outer part of the visual disk. This is mainly due to the very low surface brightness and the limited field sizes available (mosaics are difficult to combine at the required level of accuracy). As important stellar resonances such as the co-rotation in many cases are expected to be in the outer disk of normal spiral galaxies, the study of the outer regions is required for a better understanding of amplification mechanisms of density waves.

4.3.3 Star formation

Although less spectacular than merger driven star formation at early epochs, star formation in disks of galaxies is important for their chemical evolution. The process of star formation is still not full understood. Nearby galaxies provide a very good laboratory to study the large scale properties of star forming regions. The relative importance of star formation triggered by large scale shocks in the gas (e.g.due to density waves) and stochastic formation is not clear. It will be possible to observe maps of molecular gas in nearby galaxies with resolutions down to $\sim 0.1''$ when ALMA becomes operational around 2010. Combining visual, near-infrared and mm-radio maps, the relation between molecular gas, dust and newly formed stars can be observed in detail along stream lines of the gas as it moves through spiral arms. Taking NGC 2997 as an example, the K image obtained with SOFI and shown in Fig. 4.10 mainly depicts the stellar component while a (B-K) map shows the dust distribution. Besides estimating the distribution of the old stellar population from the K map (and thereby the potential perturbation of the spiral arms), one can also see a string of young stellar clusters along the spiral arms.

4.3.4 Case for HAWK-I

For the studies mentions above, one needs to observe nearby disk galaxies in the near-infrared bands. Typical nearby disk galaxies have visual diameters D_{25} in the range of 3-5'. For very deep infrared exposures, disk galaxies will only have marginally smaller diameters. A major gain in observational efficiency can be achieved if the sky background can be measured on the target frames (i.e. avoiding target-sky sequences). An 8' field would make this possible for all nearby galaxies except the ~ 10 largest galaxies. HAWK-I would thus be an ideal instrument for most of the studies described above although some



could probably be performed adequately with VISTA as an alternative. For the most detailed star formation studies in 4.3.2., however, only HAWK-I can exploit the best seeing on Paranal to match the best resolution of images at other wavelengths including the molecular maps expected from ALMA.

4.4 Galactic Star and Planetary Formation

4.4.1 Massive stars

The question of how massive stars form is one of the burning open issues in our understanding of star formation. Two major processes have been proposed: accretion through disks or coalescence of intermediate-mass stars or molecular cloud cores. We can only distinguish between these scenarios with imaging and spectroscopy of massive star-forming regions in the infrared and submillimetre wavelengths. Spatial resolution on the subarcsecond scale is required because the closest regions of massive star formation are more distant than in the case of low-mass star formation.

In addition, we do not yet know how environmental factors impact the IMF in stellar clusters where massive stars form. Answering this question requires a combination of high sensitivity and spatial resolution. These features are not provided by the VISTA survey telescope. In addition, any replacement of ISAAC should provide a larger field because regions of massive star formation are often extended over more than 5x5 arcmin. Experience with ISAAC demonstrates that the mosaicing of large fields can lead to problems, for example due to the photometric and astrometric inhomogeneity of the data.

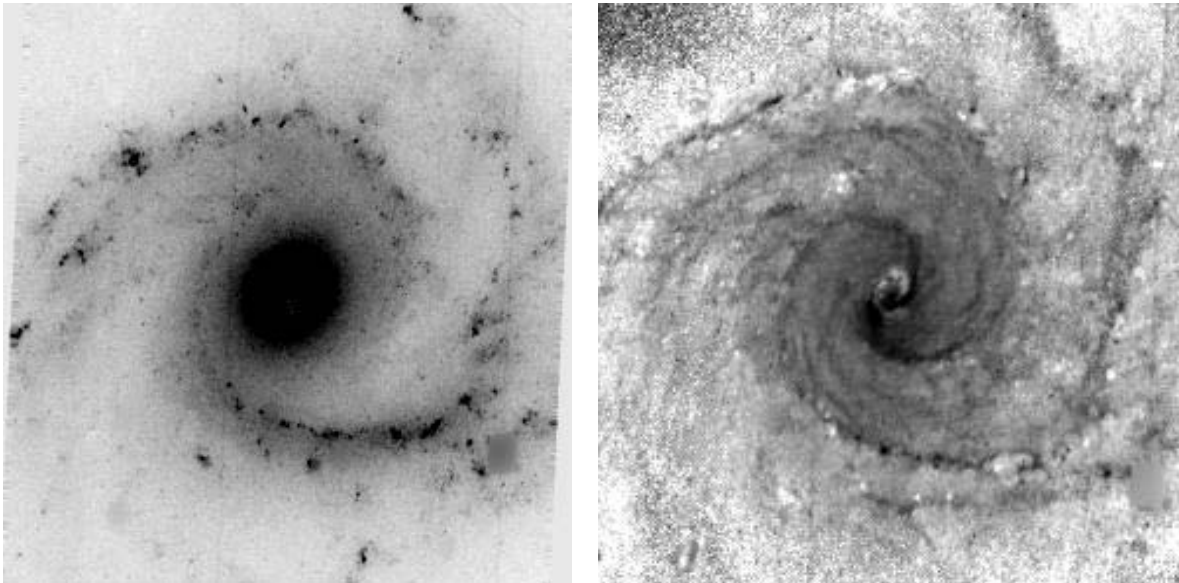
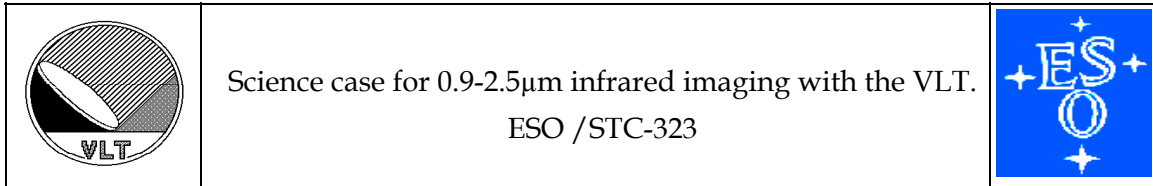


Fig. 4.10 The nearby spiral galaxy NGC 2997. Left, K band SOFI image. Right a B-K colour image.

Fig. 4.11 demonstrates that we need large fields and a pixel size adequate to well sample the intrinsic image quality. In this figure we compare the field of view (FOV) of the proposed HAWK-I camera with a relatively deep and large mosaic obtained with the



current ISAAC camera. The advantages of the larger field of view (FOV) versus a mosaicing technique are

- * Time efficiency > 13 $((8.5/2.5)^2 = 11.5$ and overlap of ~25% required between mosaiced frames.)

- * Homogeneity: increased photometric and astrometric accuracy

4.4.1.1 The impact of massive stars

When massive stars form, their intense winds and ultraviolet flux can be very destructive to the surrounding medium, creating and illuminating HII regions, as well ionising circumstellar disks around adjacent low-mass stars and thus potentially inhibiting ongoing planet formation (Bally, O'Dell, & McCaughrean 2000). In addition however, nearby molecular cloud material is first compressed before being ripped apart, and there is the possibility of new stars being formed via radiative implosion in that interlude (Larosa 1983; Bertoldi 1989; Lefloch & Lazareff 1994). It has in fact been hypothesised that most stars may form under such conditions, and thus that their final properties are as much determined by the impact of OB stars as by standard quiescent infall processes (Hester et al. 1996).

The classic test case for this scenario is M16, the Eagle Nebula, where the HST images of Hester et al. (1996) delineated three so-called elephant trunks, parsec-long columns of gas and dust being ionised by OB stars of the adjacent NGC6611 cluster. Around the fringes of the trunks, Hester et al. resolved a population of small, dense knots, which they named EGGs for evaporating gaseous globules, which Hester et al. suggested might contain young stars about to be exposed by the ionising flux of the OB stars, thus terminating accretion and helping to define their final masses.

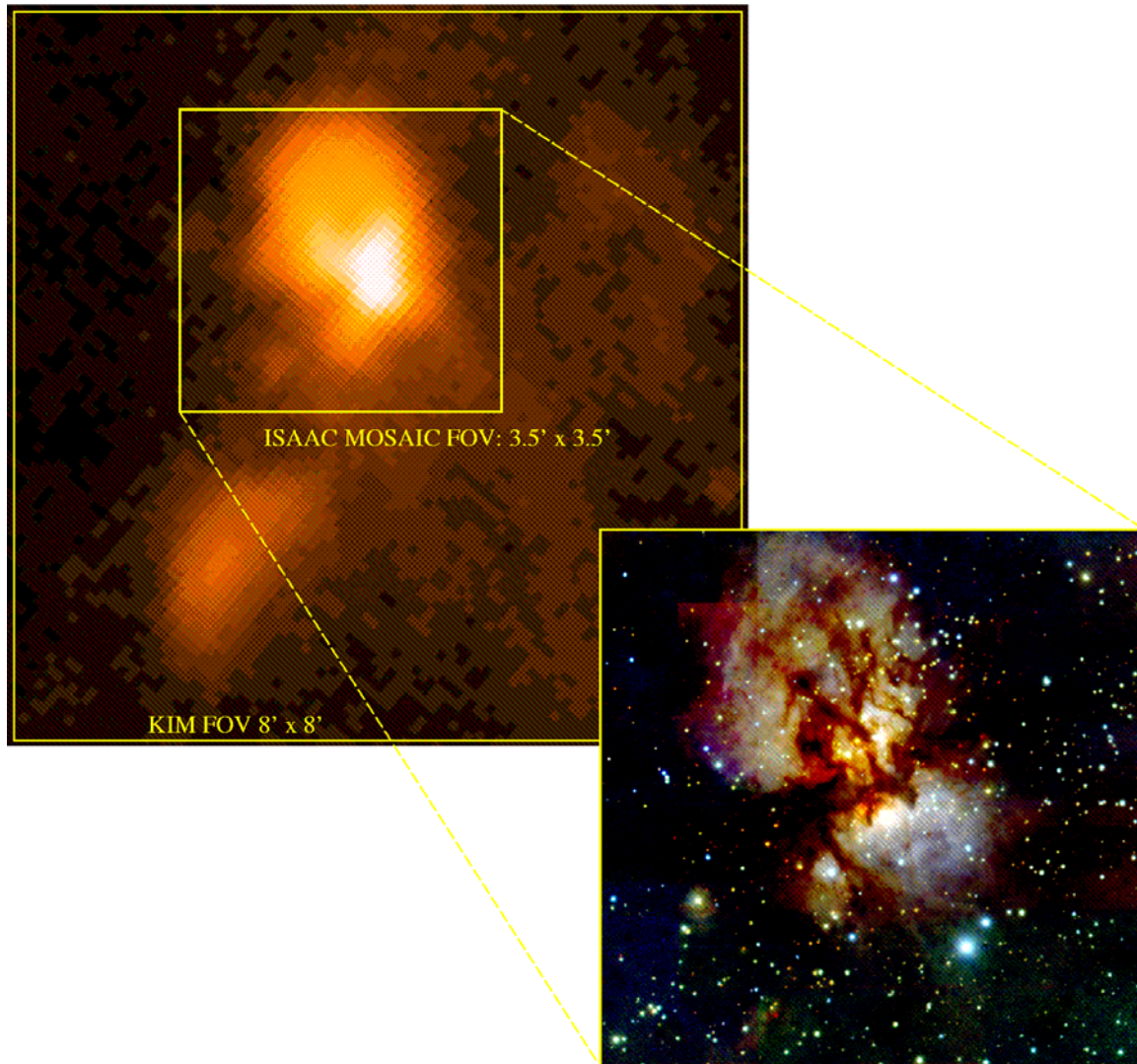


Fig. 4.11 Comparison of the field covered by a single shot of HAWK-I and an ISAAC mosaic demonstrated by the case of the massive star-forming region IRAS 09002-4732. The large-scale image is an 8.8 μ m MSX map, while the ISAAC JHK mosaic is taken from Apai et al. 2002. The 8' x 8' FOV of HAWK-I is highly efficient for deep, high resolution mapping of extended regions.

Deep, high-spatial resolution infrared observations are required in order to probe the interiors of these dense, cores in M16 and other regions with potential evidence for radiative implosion. The M16 trunks were surveyed using ISAAC with the result shown in Fig. 4.12 (see also McCaughrean & Andersen 2002; Figures 3 and 4): the experiment required excellent spatial resolution (0.35 arcsec FWHM) in order to probe the small-scale (\sim 1000AU or 0.5 arcsec) cores, but over a large field (10x10 arcmin), in order to get an accurate statistical assessment of the fore- and background field star contamination.

The point source detection limits at Js, H, and Ks of 22.6, 21.3, and 20.4, respectively, were deep enough to detect a 0.08 solar mass source embedded in 30 magnitudes of visual extinction, assuming an age of 1 Myr. Just 11 of the 73 EGGs in M16 appear to harbour

infrared sources, as marked in Figure 4.12, and thus the ongoing star formation in the trunks seems to be limited.

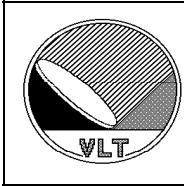


Fig. 4.12 True-colour near-infrared (1-2.5 μ m) image of the well-known elephant trunks in the Eagle Nebula, made with ISAAC. The Js data are shown as blue, H as green, and Ks as red. The cube root of the intensities were taken to compress the dynamic range before normalising and combining the three mosaics. Total integration time is 1200 seconds in Js, and 300 seconds in each of H and Ks. The seeing is 0.35 arcsec FWHM. The image covers 2.6x3.6 arcmin or 1.5x2.0pc assuming a distance of 1.9kpc to M16, and is a subsection of the full 9x9 arcmin data. North is up, East left. The small subimages each covers 18.5x18.5 arcsec (0.17x0.17pc). Labels mark evaporating gaseous globules (EGGs) identified in the optical HST data of Hester et al. (1996) found to be associated with low-mass stars and brown dwarfs. Also shown are E23, an EGG with no near-infrared point source, but thought to contain an embedded protostar driving a collimated jet; YSO1 and YSO2, massive sources in the tips of C1 and C2, respectively; and HH216, an optically-visible Herbig-Haro object (Andersen et al. 2002). (McCaughrean & Andersen (2002)).

What can HAWK-I do?

A major question remains completely unanswered however. Did these objects already exist in the trunks, only to be revealed now by the passage of the NGC6611 ionisation front, or was their formation indeed initiated by that front triggering the radiative implosion of dense cores? If the former model holds, there should be a distribution of young stars and brown dwarfs embedded within the densest parts of the trunks, not just at the ionised periphery.

In order to investigate this phenomenon in M16 and other regions with OB stars and externally ionised elephant trunks, much deeper observations are required. These must cover similarly large fields-of-view (5-10 arcmin) in order to cover all the cores and assess the field star population accurately, with excellent spatial resolution (<0.5 arcsec FWHM) in order to probe the small-scale cores. By covering the appropriate field in a single pointing, HAWK-I would avoid the need to mosaic and thus enable much deeper observations than possible with ISAAC: 2 nights of HAWK-I observations would go roughly 2 magnitudes deeper than the present ISAAC data on M16, thus making it possible to probe down a factor of 4 in mass i.e. to 0.02 solar masses, (20 Jupiter masses) in the EGGs, or to the substellar limit at 0.08 solar masses through up to 50 magnitudes of extinction in the heads of the trunks. An important side benefit of such single-pointing observations would be the more constant PSF, which leads to much more accurate PSF



Science case for 0.9-2.5 μ m infrared imaging with the VLT.
ESO /STC-323



fitting photometry than is presently possible in mosaiced surveys of extended areas in such crowded regions.

4.4.2 Dynamical studies of young, protostellar jets

Not only do high mass stars have an influence on their surrounding medium: low-mass protostars also interact with their environment via their highly-collimated jets, which remove some fraction of the angular momentum from the infalling material, and inject turbulence into the parent cloud core, perhaps clearing it and ultimately preventing further accretion.

The knotty structure of these jets implies that the central driving source is variable, with this structure providing a ticker-tape record of the accretion history of the young central protostar. Thus, proper-motion studies can be used to measure the velocities involved, making it possible to understand the timescales between accretion events, how the jet interacts and decelerates when it interacts with the surrounding medium, and what the cumulative dynamical impact on this medium is.

In young jets, typical peak outflow speeds are likely to be on the order of 100-200 km/s, equivalent to just 0.05-0.1 arcsec/yr at 500pc. It is important to measure the motions as rapidly as possible. Jets from protostars are generally bright in the $v=1-0$ S(1) line of shocked molecular hydrogen, which cools on timescales of 1-2 years. Thus, over longer timescales, there is no guarantee that it is the same packet of gas that is glowing. In addition, it is important to be able to measure velocities as low as 20 km/s, where the outflowing jet decelerates into the surrounding gas. Thus deep, wide-field, high spatial resolution images separated by 1 year or less are required.

HH212 is a well-known jet from a young Class 0 protostar, IRAS05413-0104, in Orion (Zinnecker, McCaughrean, & Rayner 1998). Seen in the shock-excited $v=1-0$ S(1) line of H₂ at 2.12 microns, it exhibits extraordinary bipolar symmetry about the driving source, with an equidistantly spaced series of knots or bowshocks on either side, extending almost 0.25pc in either direction. A proper motion study of HH212 has yielded ISAAC measurements at 4 epochs over a 24 month period in service mode, with resolution in the range 0.25-0.35 arcsec FWHM in all cases. Figure 4.13 shows a very deep (4.7 hours) stacked narrow band image, which shows the extraordinary structure of H₂ in the jet as it plows into the ambient medium, and comparison of the multi-epoch data reveal velocities of \sim 150 km/s in the inner brightest knots, with slower velocities in the outer bowshocks, as expected

Jets with HAWK-I.

HH212 is a relatively small jet, covering only 0.5pc, or 3.5 arcmin at the distance of Orion. Nevertheless, even this required mosaicing with ISAAC in order to cover it, and this mosaicing ultimately limits the accuracy that can be achieved in the proper motion measurements. Larger, older jets with different velocity structures would have to be even more extensively mosaiced, with a potentially deleterious effect on the experiment.

Thus HAWK-I, with its much larger contiguous field-of-view, would enable us to cover much larger regions of jets in a single pointing, and thus yield more accurate information to lower limiting velocities. The high spatial resolution of HAWK-I is also important as this makes it possible to measure lower velocities more rapidly, before the H₂ emission



has cooled. Finally, as shocked H₂ has a short cooling length, it is very clumpy, and the measurement of low velocities in faint features is best achieved with the extreme surface brightness sensitivity of an 8m telescope coupled with a high efficiency, high resolution camera like HAWK-I.

4.4.3 Measuring and understanding the Initial Mass Function (IMF)

It is well known that the entire life history of a star is almost uniquely determined by its mass, and yet it remains quite unclear how a star arrives at that mass in the first place. In a more general sense, we do not know how to predict the distribution of masses of a population of stars recently born from a molecular cloud, as found in a young cluster, for example, the initial mass function (IMF).

By measuring the form of the IMF and its high- and low-mass cutoffs as a function of environment, including metallicity, cluster density, presence of massive stars, for example, we can hope to place important constraints on any general theory of star formation. The single power-law form of the upper IMF in our galaxy is well-known (Salpeter 1955), but at lower masses, there is a turndown and peak in the IMF somewhere in the range 0.1-0.5 solar masses, just above the stellar/sub-stellar break (Kroupa 2001).

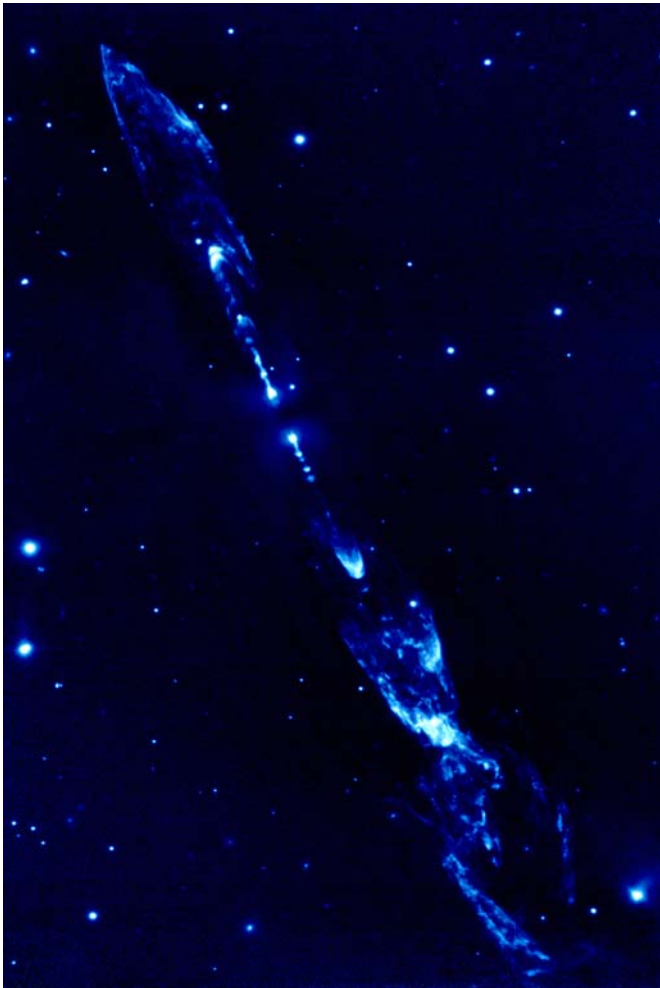
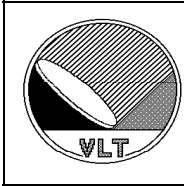


Fig. 4.13 A deep image of the protostellar jet, HH212, in the 2.122 micron $\nu=1-0$ S(1) line of molecular hydrogen, made using ISAAC on Antu, with data from October 2000, October 2001, and January 2002. North is up, east left. Total integration time in the central half is 282 minutes, yielding a 3 sigma per pixel limiting surface brightness sensitivity there of $1.2 \times 10^{-19} \text{ W m}^{-2} \text{ arcsec}^{-2}$. The image covers 3.2×3.9 arcmin or 0.37×0.45 pc assuming a distance of 400 pc to HH212. The resolution is seeing limited at 0.34 arcsec FWHM. Intensities have been scaled logarithmically. Continuum emission has not been subtracted as the jet is known to be emitting almost exclusively in the S(1) line: however, continuum sources such as field stars and galaxies remain visible. (From McCaughrean et al. (2002)).

The form of the IMF over this peak and down into the brown dwarf regime must encode important physics, particularly as the lower-mass cutoff is reached. The theory of hierarchical fragmentation predicts that a collapsing molecular cloud will continue to break into ever smaller clumps as long they are able to radiate away their excess energy in less than the free-fall time for local collapse. However, opacity rises with density, and at some point the gas cannot cool quickly enough, it becomes adiabatic and pressure-supported, and fragmentation ceases (Hoyle 1953). Traditionally, this lower cutoff is predicted to lie at 0.005-0.015 solar masses or 5-15 Jupiter masses (1 Jupiter mass = 0.001 solar mass) (Lynden-Bell & Low 1976; Rees 1976; Silk 1977), although more recent calculations suggest that it may be modified by the inclusion of magnetic fields, down to perhaps as little as 1 Jupiter mass (Boss 2001).

More importantly, however, the whole fragmentation scenario down at low masses may have to be replaced by a more complex model involving a wide range of physical processes, including supersonic turbulence (Padoan & Nordlund 2002), dynamical interactions between protostars (Bate, Bonnell, & Bromm 2002), and feedback due, for example, to strong bipolar outflows (Adams & Fatuzzo 1996) and ionising radiation from



massive stars (Palla & Stahler 2000). In addition, the existence of such objects with just a few Jupiter masses would be interesting in itself, as they could serve as surrogates for true planets, and provide important insights into their very early evolution.

4.4.3.1 A case study - the Orion Nebula

Such Jupiter mass objects are relatively bright when young, and deep infrared imaging can be used to locate them in nearby star-forming regions. One key site for such observations is the young (1 Myr), dense (50,000 stars per cubic parsec core density) Trapezium Cluster in Orion, which has proven an excellent site for probing the stellar IMF (Hillenbrand 1997) and is known to contain many brown dwarfs down to perhaps even 10 Jupiter masses (McCaughrean et al. 1995; Luhman et al. 2000; Hillenbrand & Carpenter 2000; Muench et al. 2001; Lucas & Roche 2000; Lucas et al. 2001).

The deepest, wide-field survey to date has been made with ISAAC on Antu, covering a 7x7 arcminute field centred on the well-known Trapezium OB stars, and shown in Fig. 4.14 (McCaughrean et al. 2001, 2002). The survey has 900 seconds integration time pixel per filter, with a mean seeing of 0.5 arcsec FWHM. These data reach 3 sigma peak-pixel point source detection limits in Js, H, and Ks of 21.3, 20.0, and 19.6, respectively, limits ultimately set by the bright emission from the Orion Nebula. In the Ks band, these limits correspond roughly to 3 Jupiter masses at 450pc, assuming an age of 1 Myr and a typical intracluster reddening of $A_v=7$, using the DUSTY pre-main sequence models of Chabrier et al. (2000).

There are roughly 1200 sources in the survey region, 700 fainter than the saturation limit of $K_s=13$, and the Js-H vs. H colour-magnitude diagram is shown in figure 4.15. The diagram shows how an extinction-limited sample of stars can be drawn covering the mass range 5-80 Jupiter masses, and how a two point mass function can be derived covering the brown dwarf regime, with $dN/d \log M \propto M^{-1}$; this should be contrasted with the classical Salpeter mass function in the stellar domain which goes as $\propto M^{-1.35}$.

Thus, the mass function is falling steeply through the brown dwarf regime, with rather few sources below 5 Jupiter masses. It is thus possible that these data are approaching a lower-mass cutoff in the IMF, but significantly deeper imaging is required to probe below the present limits, to ensure that any such boundary is delineated on a statistically sound basis. Furthermore, uncovering sources in the 1-3 Jupiter mass range would prove very significant in the characterization of young giant planet analogues.

4.4.3.2 Deeper into Orion with HAWK-I

Pushing the present extinction-limited sample complete to 5 Jupiter masses down a factor of two in mass is challenging. Using the COND and DUSTY models of Baraffe, Chabrier, Allard, et al., a 2.5 Jupiter mass source at 1 Myr is roughly 1.5 magnitudes fainter than its 5 Jupiter mass counterpart in both H and Ks, and thus integration times roughly 16 times longer than present would be required, i.e. 4 hours on-source integration time per filter per field-of-view. With ISAAC, such an experiment would be prohibitive: the present survey required a mosaic of 9 positions to cover the cluster core and yield a statistically significant sample, and including all overheads, 3 nights of good observing weather. Going down a factor of two in mass over the same field with ISAAC would cost almost 50 nights.



Science case for 0.9-2.5 μ m infrared imaging with the VLT.
ESO /STC-323



Fig. 4.14 A true-colour near-infrared (1-2.5 μ m) image of the Orion Nebula and Trapezium Cluster made using ISAAC on Antu in December 1999 (McCaughrean et al. 2001). The J_s data are shown as blue, H as green, and K_s as red. In this representation, cube root intensities were used to compress the dynamic range. The image covers 7 \times 7 arcmin, or 0.9 \times 0.9pc at the 450pc distance to the nebula. North is up, east left. Total integration time in this subset of the data is 270 seconds per filter, and the seeing is 0.5 arcsec FWHM.

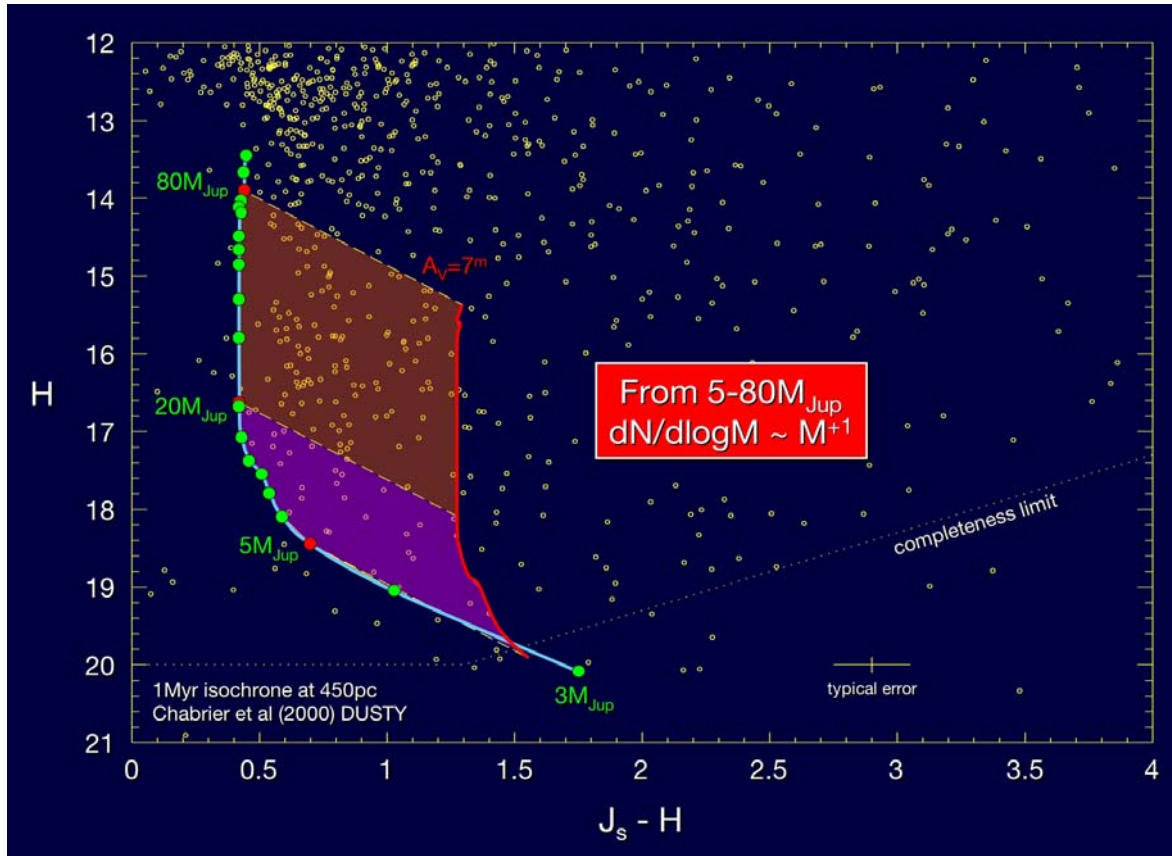


Fig. 4.15 The J_s - H vs. H colour-magnitude diagram derived from the deep ISAAC imaging survey of the Trapezium Cluster (Fig. 4.14). The completeness limit and typical photometric errors for sources just above this limit are shown. The 1 Myr isochrone from the pre-main sequence (DUSTY) models of Chabrier et al. (2000) is plotted assuming a distance of 450pc. The great majority of the sources lie redwards of the isochrone due to intracluster dust extinction of up to 20 magnitudes and greater. There is a pileup of sources at $H=12-13$ due to the effects of deuterium burning, although sources brighter than this saturated within the 10 second on-chip integration time used for the survey. The number of potential brown dwarfs is large, but not dominant. The 0.005-0.08 solar mass (5-80 Jupiter mass) segment of the isochrone is shown, reddened by $A_v=7$: by counting sources in the 5-20 and 20-80 Jupiter mass bins, the brown dwarf end of the IMF is seen to be falling as $dN/d \log M \propto M^{+1}$.

With HAWK-I, just a single pointing would be required, and this experiment would be readily tractable in just a couple of nights. Furthermore, it would then be possible to carry out similar surveys in a number of nearby star-forming regions, to test whether or not the lower-mass cutoff in the IMF varies with environment. Typical young embedded clusters have the bulk of their members within a 1 parsec diameter region, i.e. 7 arcmin at 0.5kpc, and thus almost always covered by a single pointing of HAWK-I.

In this light, it is important to realize that the non-contiguous field of VISTA would be entirely unsuited to this sort of experiment: for a single contiguous field, HAWK-I would always be much more efficient. In addition, the seeing-limited sampling of HAWK-I is



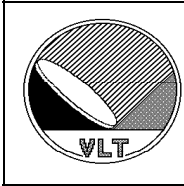
vital in order to enable the detection of faint point sources against the bright nebulosity of the surrounding HII region: the coarse VISTA sampling is again unsuitable.

4.4.3.3 The lowest end of the mass function in nearby star forming regions

The search for the bottom of the stellar mass function, one of the main goals of surveys of star forming region less than one decade ago, has been replaced in recent years by the search for objects beyond the bottom of the *brown dwarf* mass function. The realization that freely-floating objects keep being found as surveys probe lower and lower masses has forced us to rethink object formation theories and even basic definitions, giving rise to a plethora of new denominations (low-mass brown dwarfs, IPMOs, fusors, planemos, free-floating planets...) that basically define objects not orbiting a larger body and whose mass is near or below the deuterium-burning limit, set by theoretical models at 13 Jupiter masses. We adopt henceforth the denomination IPMOs (Isolated Planetary-Mass Objects) to refer to objects below this limit, and more specifically YIPMOs (Young IPMOs) to refer to those found in star forming regions.

YIPMOs with a few Jupiter masses should have temperatures below 2000K and spectral characteristics similar to those of field L-type dwarfs, characterized by very red intrinsic colours at both visible and infrared wavelengths due to the low temperatures and the abundance of dust in their atmospheres. Successful searches for YIPMOs in this range have been made at visible wavelengths with wide-field imagers at moderately large telescopes, and have provided some detections with estimated masses down to about 5 Jupiter masses. The search for even less massive YIPMOs (of one Jupiter mass and below) is more challenging, since at the distance of even the nearest star forming regions such objects are too faint to be detected in the visible. However, they are relatively accessible in the infrared: at a distance of 150 pc, a 1 Myr old Jupiter-mass YIPMO should have $H \sim 19$ and distinctive “blue” colours in the infrared ($J-H \sim 0$, $H-K \sim 0$) and even bluer as temperatures drop below 1000 K due to dust sedimentation below the photosphere and flux redistribution due to the opacities of the molecules present in the atmosphere. Some expected $H \nu$ $H-K$ tracks and the possible detection of a YIPMO in the Chamelion I star forming region with ISAAC (Comerón, 2001) are shown in Fig 4.16. Detecting Jupiter- and sub-Jupiter-mass YIPMOs is thus in principle within the reach of current instrumentation at a large telescope, but the combination of depth and sufficiently large field for an effective blind search in regions having typical sizes of at least a fraction of a square degree can be offered only by an instrument like HAWK-I at the VLT.

Estimating the actual depth in terms of detectable mass that HAWK-I could reach is a difficult task, since one needs to venture into a region of the mass-age parameter space that is so far uncharted both by observations and by theoretical models. The difficulties encountered in modeling YIPMOs of Jupiter and sub-Jupiter mass at ages of a few million years are quite formidable – complex and interlinked aspects such as the early evolution of temperature, surface gravity, convection structure, and dust formation and settling play a dominant role in determining the appearance and evolution of the object. The difficulties in predicting the numbers of such objects that could be found are also important, since even the basic formation mechanism for the known YIPMOs (formation in isolation vs. ejection from a protoplanetary system) is still controversial. However, current models



suggest that a detection limit of $H=24$, $K=24$ could allow the detection of even sub-Saturn mass YIPMOs.

Deep surveys with HAWK-I will thus have to first answer the most basic question about sub-Jupiter-mass YIPMOs - namely, whether or not they exist. Both their detection and their non-detection will have important consequences on object formation theories at such low masses. Assuming that they do exist, their observation will provide the first hints at their actual spectral energy distribution, much more precisely than models can predict in the near future. The detection and observational characterization of Jupiter- and sub-Jupiter-mass YIPMOs can be expected to trigger a vigorous activity in theoretical research and large observational efforts to enlarge the sample of such objects.

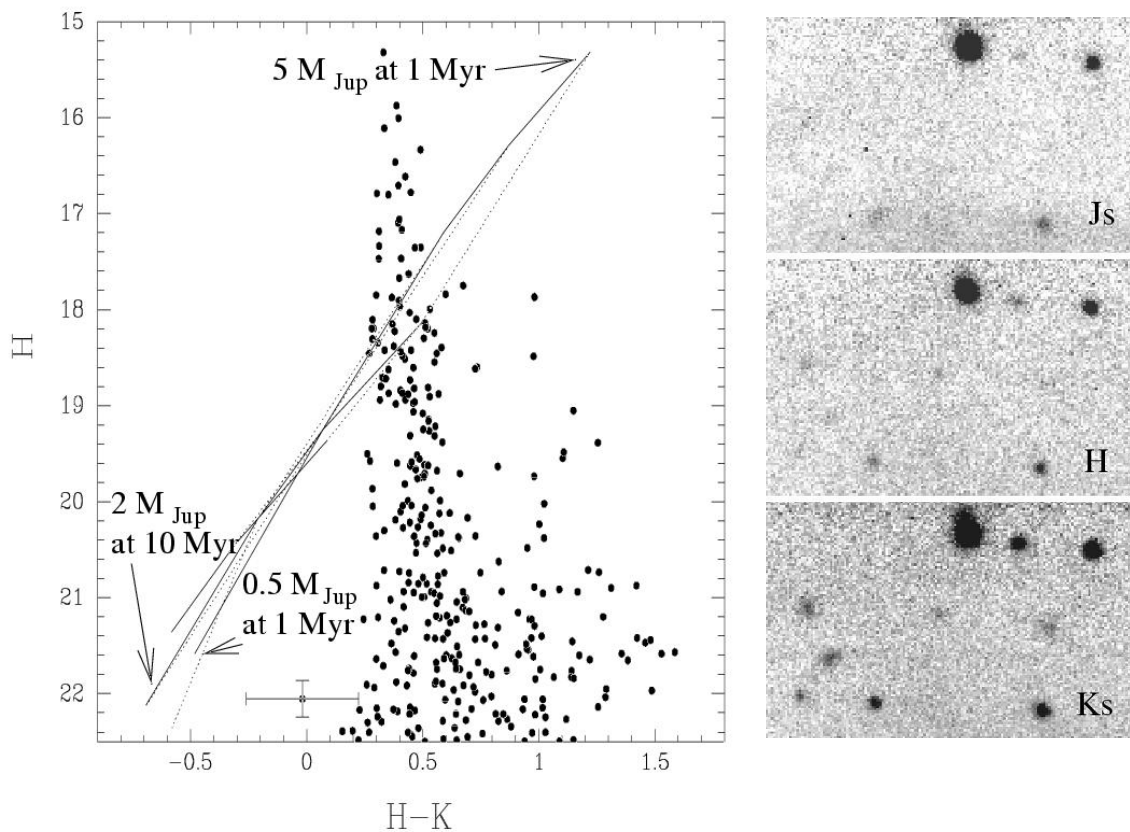


Fig. 4.16 Low mass objects detected with ISAAC in the Chameleon I star forming region (Comerón, 2001). The candidate YIPMO is marked in the lower left corner and its discovery images are shown in the right hand panel.

While follow-up spectroscopy of the brightest YIPMOs in the Jupiter-mass range may be feasible with 2nd generation VLT instruments like X-shooter (as well as with ISAAC, in case it is still in operation when HAWK-I comes on-line), much spectral information of great constraining value for models can already be gained from medium-band imaging. Spectral features produced by the dominant molecules in the JHK bands are both prominent and broad, and provide in fact powerful search criteria based on exotic medium-band colour criteria. Therefore, HAWK-I will be sufficient to provide both



detections and meaningful spectral information. Over a sufficiently long timescale (5-10 years), HAWK-I will also provide very valuable kinematical (proper motion) information - an as yet unexplored aspect of YIPMO research that has primordial importance on testing the isolated vs. ejected formation scenarios.

4.4.3.4 Starbursts and dependence of the IMF on environment

The concept of an initial mass function (IMF), which is independent of the environment or the epoch of star formation was introduced by Salpeter and Sandage in the 1950s. Soon after its inception, the universality of the IMF was questioned. The notion that high-mass stars might suppress the formation of low-mass stars, or that regions with very high star formation rates might be deficient both in very high-mass and low-mass stars became a common concept. The starburst galaxy M82, which is the best studied example for starbursts on a galactic scale, is often cited as a prime example. Despite intensive studies, however, the evidence for the presence (e.g., Puxley 1991; Doane & Mathews 1993; Rieke et al. 1993) or absence (Satyapal et al. 1997) of a mass cut-off in M82 remains inconclusive.



Science case for 0.9-2.5 μ m infrared imaging with the VLT.
ESO /STC-323



Fig. 4.17 Composite colour JHK ISAAC image of NGC 3603. The insert on the lower right shows a zoom-in on the central cluster (Brandl et al. 1999).

The galactic giant HII region NGC 3603 has about 100 times the luminosity of the Orion nebula, and about 10% of the luminosity of 30 Doradus, which in turn is the most luminous HII region in the Local Group of galaxies (Kennicutt 1984). Because of its large extent of (at least) 30 arcmin, a complete census of NGC 3603 stellar (and substellar) population, and hence its mass function is still missing. The 2MASS and DENIS surveys are too shallow, and lack spatial resolution to resolve the intermediate to low-mass stellar and substellar population. The deep VLT/ISAAC pointing shown in Fig. 4.17 was

obtained under excellent seeing conditions (<0.4 arcsec) and covered the central 3.4×3.4 arcmin (Brandl et al. 1999). The colour - magnitude diagrams shown in Fig. 4.18 contain close to 7000 stars and comparison with theoretical pre-main-sequence isochrones indicates that objects with masses down to at least 0.1 solar masses, i.e. close to the hydrogen burning limit, are detected in the cluster (Brandl et al. 1999).

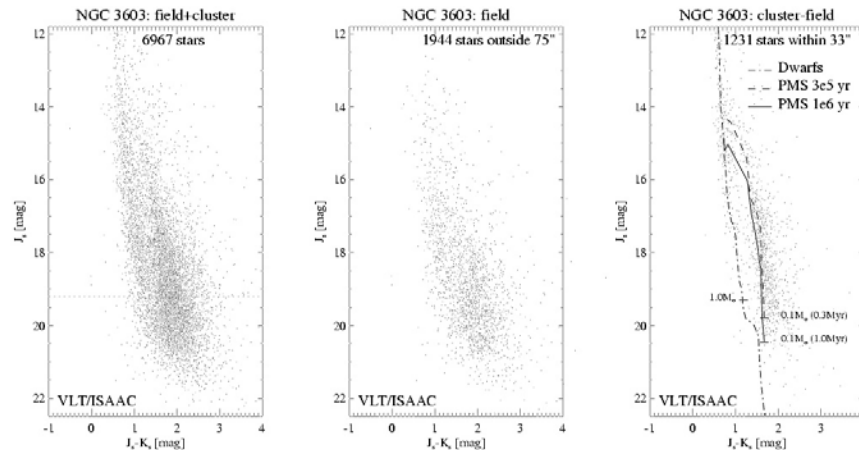


Fig. 4.18 J vs. J-K colour-magnitude diagrams of the NGC 3603 region as observed with ISAAC. Close to 7000 stars could be identified (left). Comparison with theoretical pre-main-sequence isochrones indicates that objects with masses down to at least 0.1 solar masses, i.e. close to the hydrogen burning limit, are detected in the cluster (Brandl et al. 1999).

A comprehensive study of the stellar (and substellar) population of NGC 3603 however would require a much large field coverage as indicated in Figure 4.19.

A wide field NIR imager adapted to the high spatial resolution provided by VLT could easily carry out a complete census of the stellar population in the NGC 3603 HII region and other Galactic and Local Group starburst regions like 30 Doradus, and extend our knowledge of the mass function down to very low-mass (including the substellar regime for many of the Galactic regions).

Covering such large areas with ISAAC (or especially NACO) would be prohibitive because of the smaller field of view, and hence the huge amount of telescope time required.

4.4.4 Deep, wide field NIR survey for edge-on circumstellar disk sources.

The coplanarity of planetary orbits in the solar system led Kant (1755, Allgemeine Naturgeschichte und Theorie des Himmels) to the suggestion that the solar system evolved out of a flattened, disk like structure ("Urnebel"). In the past ten years the use of new telescopes and instrumentation as well as improvements in theoretical modeling have provided strong support for Kant's Urnebel hypothesis. HST detected silhouette disks in the Orion Trapezium cluster (McCaughrean & O'Dell 1996), and bipolar reflection nebulosities and dark lanes (interpreted as disks seen close to edge-on) in the Taurus T association (e.g., HH 30 (Burrows et al. 1996); IRAS 04302+2247 (Padgett et al. 1999)). Edge-on disk sources were also identified in the rho Ophiuchi star forming regions with

the VLT and ISAAC as shown in Fig. 4.20 (Brandner et al. 2000; Grosso et al. 2003). Disks seen close to edge-on are of special interest as they act as natural coronagraphs by blocking the light from the central star. The spatially resolved observations of circumstellar disks made it possible to derive physical disk parameters like size, scale height and degree of flaring, or density and temperature structure.

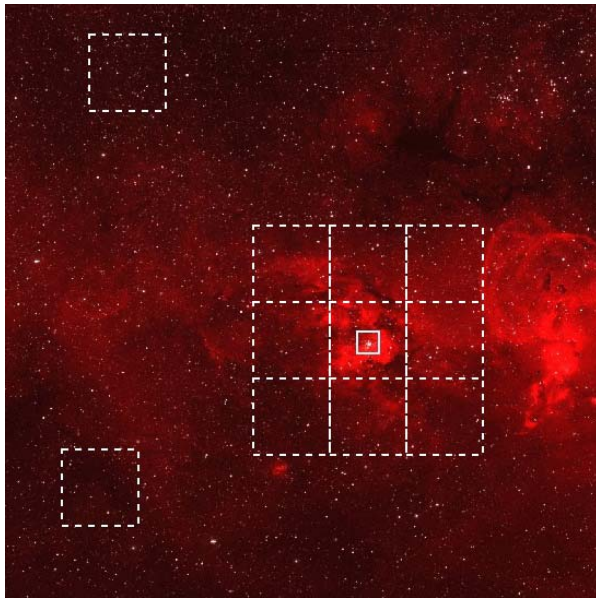


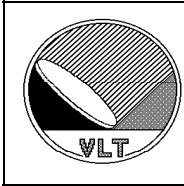
Fig. 4.19 The Galactic Giant HII region NGC 3603 with its central starburst cluster viewed in H-alpha with the Curtis-Schmidt telescope. The field of view is 1.1deg x 1.1 deg. The ISAAC field of view, (solid line), and the location of a 3 x 3 HAWK-I mosaic (dashed lines) plus two off-fields are indicated. 122 VLT/ISAAC pointings would be required to cover the same area as the 11 HAWK-I pointings.

Up to now, only of the order of 10 clear-cut cases for edge-on disk sources have been identified in the nearby star forming regions of Taurus and Ophiuchus. These sources are at various stages of evolution, with estimated masses for the central stars in the range of 0.2 to 2 solar masses, and ages between a few 100,000 yr to several Myr. More sources are needed in order to develop a comprehensive picture of the physical and chemical processes taking place in circumstellar disk, which ultimately might lead to the formation of planetary systems.

A study by Thornley et al. (2000) indicates that the high-mass stellar content in starburst galaxies is similar to local starburst events. Thus local starbursts should constitute excellent laboratories to learn about the physical conditions in starburst galaxies.

Assuming a random orientation of circumstellar disks, 10% to 15% of all Young Stellar Objects (YSOs) should be seen with their circumstellar disks close to edge-on. Surveys of all nearby YSOs, however, revealed less than 5% edge-on disk sources. This indicates that the majority of edge-on disk sources is still missing (most likely due to their relative faintness in the NIR) in our census of nearby YSOs.

A wide field NIR imager adapted to the high spatial resolution provided by VLT would be the ideal tool to carry out a deep, wide-field survey for faint Class I sources and edge-on circumstellar disk sources in the nearby (<150 pc) low-mass star forming regions of Chamaeleon, Ophiuchus, Lupus, and Corona Australis, which all span one to several



degrees on the sky. Assuming a total of 300 to 400 Class I sources and classical T Tauri stars in these regions, the survey would reveal 30 to 55 new edge-on disk sources.

All newly discovered edge-on disks could be followed-up at still higher angular resolution using ground-based adaptive optics in the NIR, and mm-interferometry (with ALMA) in the radio domain. The complete data sets can then be compared to theoretical models of circumstellar disks. This comparison will yield the basic physical parameters of the circumstellar disks like their sizes (radial and vertical extent), mass and density structure, or dust and chemical composition. A precise knowledge of these properties is a pre-requisite for a better understanding of the astrophysical processes involved in the formation of planetary systems

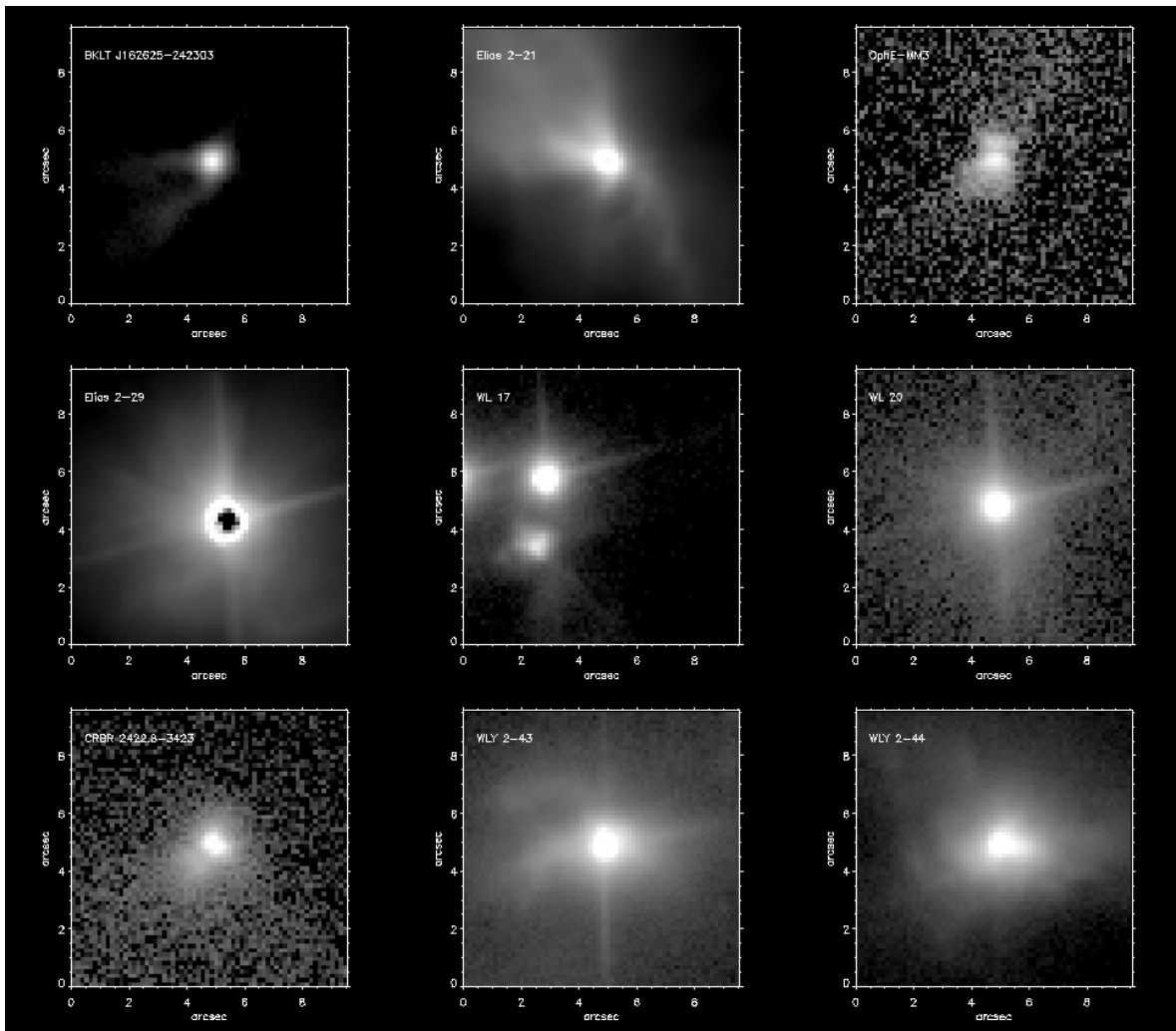
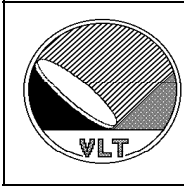


Fig. 4.20 Examples of YSOs with circumstellar material (including two edge-on disk sources from Brandner et al. 2000) identified in just 3 VLT/ISAAC fields in the rho-Ophiuchi region. The



excellent image quality with a FWHM of 0.35 to 0.40 arcsec was a pre-requisite for the direct detection of the faint circumstellar reflection nebulae.



Science case for 0.9-2.5 μ m infrared imaging with the VLT.
ESO /STC-323



4.5 Outer Solar System Bodies

4.5.1 Surveys

Surveys for outer solar system bodies will probably mostly continue to be conducted in the V or R bands where the solar spectrum peaks and the object/sky contrast is best. Looking maybe a bit far in the future (2015), one possible driver for a deep infrared survey capability is the Pluto-Kuiper Express space mission which will travel to Pluto, and then is expected to be re-routed toward a (or various) TNOs located behind Pluto. Integrating backward the orbits of these objects to the present date indicates that these targets are currently located very near to the galactic center, where traditional optical search methods are very inefficient. For such a survey, infrared sensitivity and the largest possible field (ideally $> 15''$) would be the most critical characteristics.

4.5.2 Photometry of distant, icy, minor bodies:

Transneptunian objects (TNOs) and other related minor bodies (Centaur, Plutinos, and Comets) are icy remnants of the early Solar System. The largest reservoir of such objects is the Edgeworth-Kuiper (EK) Belt (located at heliocentric distances, $r > 30\text{AU}$); it contains about 10^5 objects with diameters larger than 100km, and a total mass of about 0.1 earth masses. The Plutinos (named after Pluto, the brightest Plutino) are objects from the EK Belt that have been trapped in mean-motion resonance with Neptune. While the current members of the EK Belt are dynamically stable over the age of the Solar System, a small fraction of that population can escape, either as the result of collisions or strong, random interaction with some of the outer planets. These end up on very eccentric orbits, forming the dynamically unstable population of the "Centaur" (with a typical life-time of 10^6 yr). Some of these ejected TNOs can also end up on orbits taking them at small heliocentric distances, where their volatile components sublimate; they become then Short Period Comets. For completeness, Long Period Comets come from another reservoir, the Oort cloud, located at 10^4 AU from the Sun which, in turn, would have been populated at the time of the planet formation by planetesimals originating in the Uranus-Neptune region.

While this dynamical cascade is now fairly well understood, the physical properties of these minor bodies are still very poorly known. Indeed, their typical R mags are in the 20 - 25 range, with R-K in the 1-2 range, which makes their spectrophotometric study challenging, even with VLT-class telescopes. About 100 of them have been observed photometrically in the visible, but no more than 30 in the near-IR, and only a handful have simultaneous Vis-IR photometry. It is now clear that 1) these objects present a broad diversity of colours, which is currently interpreted as the result of evolution/aging processes (irradiation, which cause a reddening of the surface by de-hydrogenation and carbonization of the upper layer of the object, and collision and cometary activity, which rejuvenate the surface by exposing and/or depositing fresh material from the interior on the surface), 2) Vis-IR colours are the ones which give the richest and most constraining information on these processes. However, because of their irregular shape, possible variegated surface, and possible transient phenomena, many TNOs present brightness variations with an amplitude of up to 0.7mag, and rotational periods of 3-8h. It is therefore essential to obtain these Vis. and IR measurements simultaneously, a task that only the VLTs can achieve easily, one of the UTs observing them in the visible, the other in the N-IR.



Science case for 0.9-2.5 μ m infrared imaging with the VLT.
ESO /STC-323



The requirement for a near IR camera to perform these observations are the following:

- Field of view: > 2 arcmin are needed in order to securely acquire the object (orbital uncertainties for "secure" object can be up to 30") and to provide a good set of reference stars for PSF comparison as well as monitoring and fine correction of the photometry.
- Filters and wavelength range: JHK (or Ks) for broad-band studies, which provide the minimum data set. In a second step, a set of medium/narrow-band filters centered on various absorption lines of geological interest could be used, e.g. for the determination of Water Ice abundance -although this will have to be restricted to the brightest objects in the population. As a reference, the current SOFI/ISAAC filter set contain several NB filters that are useful for this kind of observations.
- Pixel size: not critical, provided that the PSF is adequately sampled.

4.5.3 Size distribution of Long Period Comets.

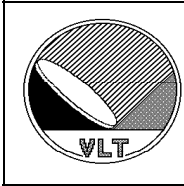
The size distribution of Short Period Comet (SPC) nuclei and of their progenitors, the Centaurs and TNOs, has begun to be established. For the SPCs, most of the data are acquired when the comets are distant enough from the Sun to be inactive (i.e. not surrounded by a coma), or using HST for an accurate modeling and subtraction of the coma when they are very close to the Sun (both methods give similar results). These size distributions are of importance to characterize the accretion processes forming these objects, and then the collisional evolution they suffered.

On the other hand, the size distribution of Long Period Comet (LPC) nuclei is absolutely unknown. As these objects were ejected from the Uranus-Neptune region at the time of the accretion of these planets, they preserve important information on the conditions prevailing at that time in these regions, which in turn is needed in order to understand the planetary formation processes.

A problem with LPCs is that their super-volatile content (i.e. CO, CO₂ and other species that can sublimate at very low temperature) is much higher than that of the SPCs. As a consequence, they remain active at very large heliocentric distances, the coma hiding the nucleus. Various attempts to observe the nucleus have been performed with Keck and HST but in no case could the nucleus be detected. Even taking into account the contamination by the coma, this implies that these nuclei are very small (typically <1km). The only firm detection of an LPC nucleus has been achieved on Comet Hyakutake, resulting in a very small nucleus of ~0.1km rad.

A possible way to solve this question would be to observe LPCs in the NIR, where the contrast between the nucleus and the dust is higher than in the visible. The observations should be performed at intermediate heliocentric distances (> 5AU, where the water-ice sublimation is stopped) and where a small nucleus can still be detected. A careful modeling and subtraction of the coma contribution will lead to an estimate of the flux from the nucleus, and thereby of its size.

It is important to note that a classical instrument, as opposed to an adaptive optics (AO) one, is preferred. Indeed, the PSF of an AO system is constituted by a diffraction limited core surrounded by a wider halo. This looks dangerously like a comet nucleus surrounded by a faint coma. The fraction of the light in the halo varies with the quality of the AO correction, which is not necessarily stable. It is therefore very difficult to disentangle the



coma contamination and the nucleus light in the halo, resulting in large uncertainties that cancel out the advantage of using an AO system.

The requirement for a near IR camera to perform these observations are the following:

- Field of view: at least 2-3 arcmin are needed in order to acquire the comet, have enough field for registering the coma far enough from the nucleus for proper modeling, and to provide reference stars for PSF analysis.
- Pixel: a good oversampling of the PSF is required for proper modeling.
- Filter: standard JHK.

5. References

- Adams, F. C. & Fatuzzo, M. 1996, *ApJ*, 464, 256
- Alves, J. & McCaughrean, M. J. 2002, eds. *The Origins of Stars and Planets: The VLT View*, (Berlin: Springer Verlag)
- Andersen, M., Reipurth, B., Knude, J. et al. 2002, *A&A*, in press
- Apai, D., Henning, T., Stecklum, B.: 2002, *Proceedings of Hot Star Workshop III*. ASP 267, 337
- Bally, J., O'Dell, C. R., & McCaughrean, M. J. 2000, *AJ*, 119, 2919
- Bate, M. R., Bonnell, I., & Bromm, V. 2002, *MNRAS*, 332, L65
- Bertoldi, F. 1989, *ApJ*, 346, 735
- Blandford 2001, "The Future of Gravitational Optics" astro-ph/0110392
- Boss, A. P. 2001, *ApJ*, 551, L167
- Brandl, B., Brandner, W., Eisenhauer, F., Moffat, A. F. J., Palla, F., & Zinnecker, H. 1999, *A&A*, 352, L69
- Brandner et al. 2000, *A&A*, 364, L13
- Burrows et al. 1996: *ApJ*, 473,437
- Carlstrom et al. 2002, *ARAA*, 40, 643
- Chabrier, G., Baraffe, I., Allard, F., & Hauschildt, P. 2000, *ApJ*, 542, 464
- Comerón, F., 2001, *Proceedings of ESO Deep Fields Workshop*, 11
- Daddi et al., 2003, astro-ph/0303165 to appear in *ApJ*
- Doane & Mathews 1993, *ApJ* 419, 573
- Fosbury et al., 2001, *Messenger* 105, 40
- Franx et al., 2003, astro-ph/0303163 to appear in *ApJ Letters*
- Gavazzi R. et al 2003, astro-ph/0212214
- Grosso et al. 2003, *ApJ*, 586 in press
- Hester, J. J., Scowen, P. A., Sankrit, R. et al. 1996, *AJ*, 111, 2349
- Hillenbrand, L. A. 1997, *AJ*, 113, 1733
- Hillenbrand, L. A. & Carpenter, J.~M. 2000, *ApJ*, 540, 236



Science case for 0.9-2.5 μ m infrared imaging with the VLT.
ESO /STC-323



- Hillenbrand, L. A., Massey, P., Strom, S. E., & Merrill, K. M. 1993, AJ, 106, 1906
- Hoyle, F. 1953, ApJ, 118, 513
- Hu. E., et al 2002, astro-ph/0203091
- Kennicutt 1984, ApJ 287,116.
- Kurk, J., et. al.: 2002, RMAA, 13, 191.
- Labbe et al., 2002, The Messenger, 110.38
- Labbé et al., 2002; astro-ph/0212236 to appear in AJ
- Larosa, T. N. 1983, ApJ, 274, 815
- Lefloch, B. & Lazareff, B. 1994, A&A, 289, 559
- Lucas, P. W. & Roche, P. F. 2000, MNRAS, 314, 858
- Lucas, P. W., Roche, P. F., Allard, F., & Hauschildt, P. 2001, MNRAS, 326, 695
- Luhman, K. L., Rieke, G. H., Young, E. T. et al. 2000, ApJ, 540, 1016
- Low, C. & Lynden-Bell, D. 1976, MNRAS, 176, 367
- McCaughrean, M. J., Alves, J., Zinnecker, H., & Palla, F. 2001, ESO Press Photos 03a-d/01
- McCaughrean & O'Dell 1996, AJ, 111, 1977
- Mellier Y.,1999, Annu. Rev. Astron. Astrophys. 37, 127
- Moorwood, A.F.M., van der Werf, P.P., Cuby, J.G., Oliva, E.: 2000, A&A, 362, 9; 2003, Proceedings of ESO Workshop on the Mass of Galaxies at Low and High Redshift, 302
- Padgett et al. 1999, A& 117, 1490
- Puxley, P., 1991, MNRAS, 249, 11 Rejkuba et al., 2001, Proceedings of ESO Deep Fields Workshop, 32
- Rieke et al. 1993, ApJ 412, 99
- Rosati et al, 2002, ARAA, 40, 539
- Rudnick et al., 2001, AJ, 122, 220
- Satyapal et al. 1997, ApJ 483, 148
- Thornley et al., 2000, ApJ 539, 641
- van Dokkum et al., 2003, astro-ph/0303166 to appear in ApJ Letters
- White et al.,1993, MNRAS, 262, 1023.